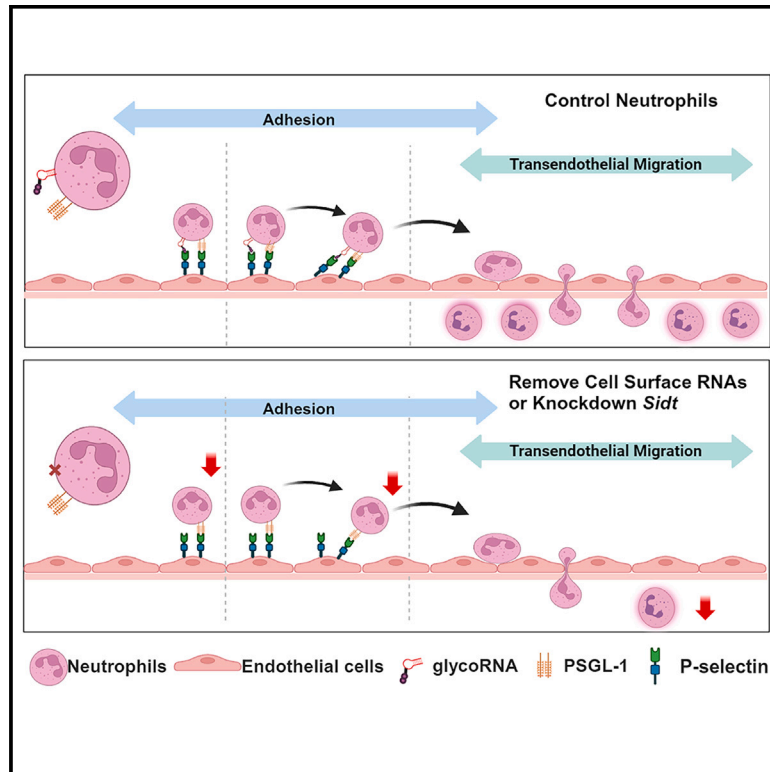


Cell surface RNAs control neutrophil recruitment

Graphical abstract



Authors

Ningning Zhang, Wenwen Tang, Lidiane Torres, ..., Andres Hidalgo, Dianqing Wu, Jun Lu

Correspondence

dianqing.wu@yale.edu (D.W.), jun.lu@yale.edu (J.L.)

In brief

RNAs present on the outer cell surface have been recently identified in mammalian cells, but the functional significance of these cell surface RNAs hasn't been clear. This study reveals roles of cell surface RNAs in mediating neutrophil recruitment to inflammatory sites in mice and the mechanisms regulating cell surface glycoRNA functions and levels.

Highlights

- GlycoRNAs are present in neutrophils and primarily locate on the cell surface
- Cell surface RNAs facilitate neutrophil recruitment to inflammatory sites *in vivo*
- Neutrophil glycoRNAs bind to P-selectin on endothelial cells
- *Sidt* genes are required for glycoRNA expression and cell surface RNA function



Article

Cell surface RNAs control neutrophil recruitment

Ningning Zhang,^{1,2,12} Wenwen Tang,^{3,12} Lidiane Torres,⁴ Xujun Wang,^{1,2} Yasmeen Ajaj,^{1,2} Li Zhu,⁵ Yi Luan,³ Hongyue Zhou,³ Yadong Wang,^{1,2,6} Dingyao Zhang,^{1,2,7} Vadim Kurbatov,^{1,2,8} Sajid A. Khan,⁸ Priti Kumar,⁵ Andres Hidalgo,^{3,9} Dianqing Wu,^{1,3,10,*} and Jun Lu^{1,2,6,10,11,13,*}

¹Yale Stem Cell Center, Yale University School of Medicine, New Haven, CT 06520, USA

²Department of Genetics, Yale University School of Medicine, New Haven, CT 06510, USA

³Vascular Biology and Therapeutics Program and Department of Pharmacology, Yale University School of Medicine, New Haven, CT 06519, USA

⁴Department of Cell Biology and Ruth L. and David S. Gottesman Institute for Stem Cell Biology and Regenerative Medicine, Albert Einstein College of Medicine, Bronx, New York, NY 10461, USA

⁵Department of Internal Medicine, Section of Infectious Diseases, Yale University School of Medicine, New Haven CT 06511

⁶Yale Cooperative Center of Excellence in Hematology, New Haven, CT 12208, USA

⁷Computational Biology and Bioinformatics Graduate Program, Yale University, New Haven, CT 06520, USA

⁸Department of Surgery, Yale University School of Medicine, New Haven, CT 06519, USA

⁹Department of Immunobiology, Yale University School of Medicine, New Haven, CT 06519, USA

¹⁰Yale Cancer Center, New Haven, CT 06520, USA

¹¹Yale Center for RNA Science and Medicine, New Haven, CT 06520, USA

¹²These authors contributed equally

¹³Lead contact

*Correspondence: dianqing.wu@yale.edu (D.W.), jun.lu@yale.edu (J.L.)

<https://doi.org/10.1016/j.cell.2023.12.033>

SUMMARY

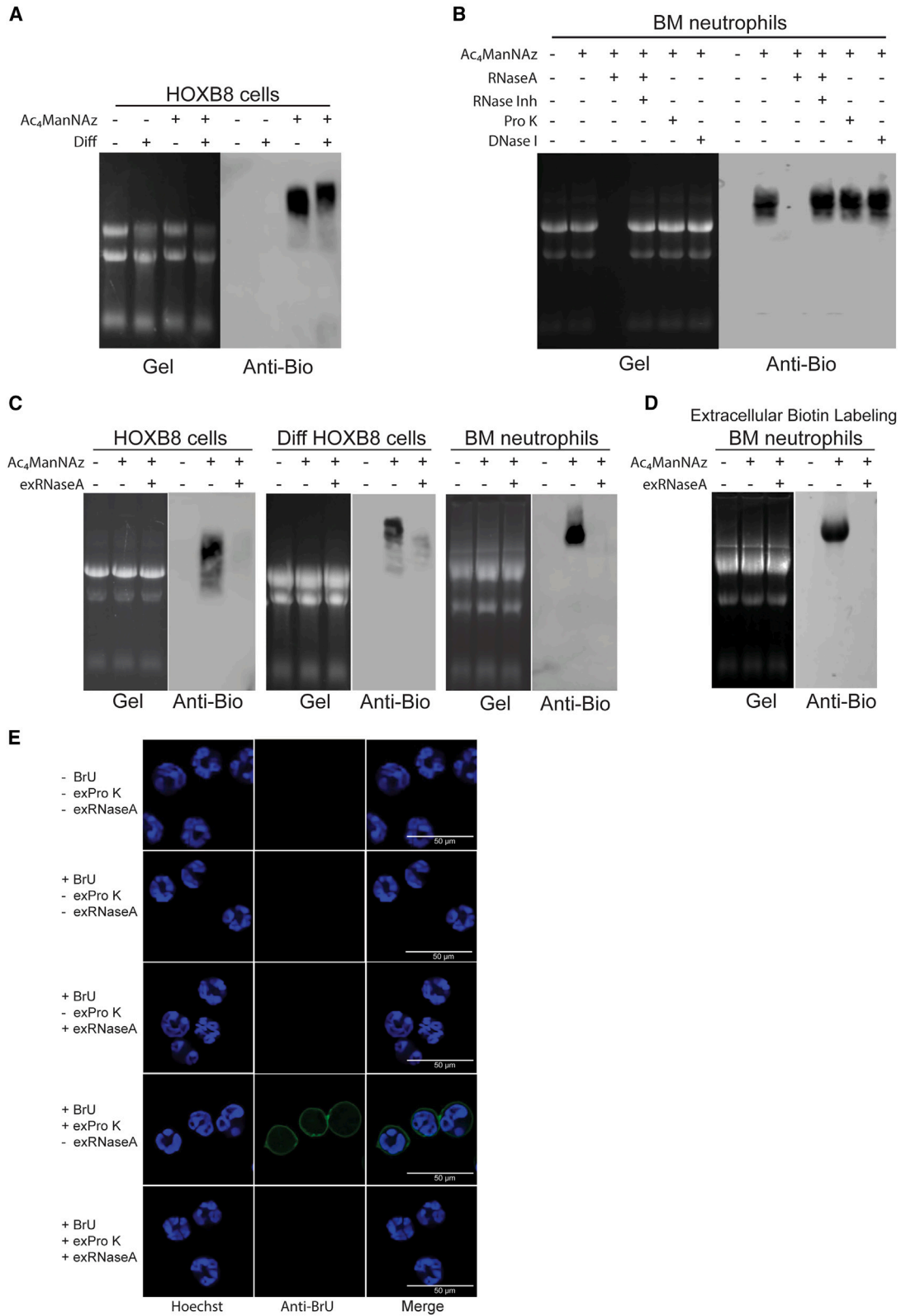
RNAs localizing to the outer cell surface have been recently identified in mammalian cells, including RNAs with glycan modifications known as glycoRNAs. However, the functional significance of cell surface RNAs and their production are poorly known. We report that cell surface RNAs are critical for neutrophil recruitment and that the mammalian homologs of the *sid-1* RNA transporter are required for glycoRNA expression. Cell surface RNAs can be readily detected in murine neutrophils, the elimination of which substantially impairs neutrophil recruitment to inflammatory sites *in vivo* and reduces neutrophils' adhesion to and migration through endothelial cells. Neutrophil glycoRNAs are predominantly on cell surface, important for neutrophil-endothelial interactions, and can be recognized by P-selectin (Selp). Knockdown of the murine *Sidt* genes abolishes neutrophil glycoRNAs and functionally mimics the loss of cell surface RNAs. Our data demonstrate the biological importance of cell surface glycoRNAs and highlight a noncanonical dimension of RNA-mediated cellular functions.

INTRODUCTION

Two recent studies detected the presence of RNAs on the outer cell surface of mammalian cells.^{1,2} Cell surface represents a topologically different space from the nucleus and cytoplasm where most cellular RNAs are located, thus raising important questions on what the functions of cell surface RNAs are and how they are produced/transported. Huang et al.¹ described a set of membrane associated extracellular RNAs (maxRNAs) in human circulating blood cells, predominantly on monocytes, and speculated that such RNA species might be captured from RNAs released from dying cells. By using antisense oligonucleotides to target specific maxRNAs, modest decreases in monocyte-endothelial adhesion *in vitro* were observed,¹ suggesting that the maxRNAs may function via unknown mechanisms that recognize their RNA sequences. The *in vivo* function of

maxRNAs, their production, and their recognition mechanism have not been identified. Flynn et al.² found that some small RNAs within cancer cell lines and embryonic stem cells contain N-glycosylation, termed glycoRNAs, with a fraction of glycoRNAs located on outer cell surface. GlycoRNAs production depends on several enzymes that also participate in protein glycosylation,² but the biological function of glycoRNAs and whether there are RNA-specific mechanisms of glycoRNA production remain enigmatic.

To address the function of cell surface RNAs, we reasoned that neutrophils are good candidates, as these innate immune cells respond quickly to tissue injuries by migrating from the circulation toward inflammatory sites, a process involving many cell-cell interactions. We therefore focused on neutrophils to study the expression, function, and regulatory mechanisms of cell surface RNAs.



(legend on next page)

RESULTS

Presence of cell surface RNAs in neutrophils

To investigate whether neutrophils contain cell surface RNAs, we first examined the presence of glycoRNAs in these cells. Initially, we utilized an *in vitro* differentiation system,³ in which primary murine bone marrow (BM) progenitors were immortalized by a *Hoxb8*-estrogen-receptor fusion gene, with differentiation induced upon removal of β -estradiol. Previous studies have shown that *Hoxb8*-immortalized cells (referred to below simply as “HOXB8 cells”) could differentiate into functional neutrophils *in vitro* and *in vivo*.^{3–7} Following the strategy of Flynn et al.,² we metabolically labeled live HOXB8 cells or HOXB8-differentiated neutrophils using N-azidoacetylmannosamine-tetracyclated (Ac_4ManNAz), which can enter the sialic acid synthesis pathway, leading to azide-modified sialic acids in glycans. Purified RNAs from labeled cells were then reacted *in vitro* with dibenzocyclooctyne-polyethylene-glycol-4-biotin (DBCO-PEG₄-biotin) via click chemistry so that sialic-acid-containing glycoRNAs could be biotin-modified. When analyzed by denaturing electrophoresis and subsequent blotting, we observed biotin signals in RNAs from both HOXB8 cells and HOXB8-differentiated neutrophils (Figures 1A and S1A). We next purified primary neutrophils (PMNs) from mouse BM (Figure S1A) and observed similar biotin signals (Figure 1B). These signals were abolished upon digestion of purified RNA by RNase A prior to electrophoresis but were insensitive to digestion by Proteinase K (Pro K), DNase I, or RNase A preincubated with RNase inhibitor (Figures 1B and S1B), arguing against the glycosylation signals being from protein or DNA contamination during RNA preparation. Additionally, the observed biotin signals had a slower migration than 28S rRNA without detectable background signals at the positions of the major rRNA bands (Figure 1B). In the absence of Ac_4ManNAz labeling, no biotin signal was observed despite the reaction of purified RNAs with DBCO-biotin (first two lanes of Figure 1A and first lane of Figure 1B). These data support that the glycoRNA signals were not due to non-specificity of the Ac_4ManNAz -DBCO-biotin labeling strategy. Together, the data above support the presence of glycoRNAs in neutrophils.

To test the presence of glycoRNAs on the outer cell surface, we treated Ac_4ManNAz -labeled HOXB8 cells, HOXB8-differentiated neutrophils, or PMNs with RNase A on live cells without permeabilizing the cell membrane. Under our extracellular RNase A (referred to below as exRNaseA) treatment condition, we did not observe major changes in rRNA bands (Figures 1C and 1D, left).

RNA sequencing (RNA-seq) performed on PMNs treated with exRNaseA showed high concordance ($R^2 > 0.99$) on the transcriptomic level with mock-treated cells (Figure S1C). Furthermore, using a non-membrane-permeable DNA dye, we did not find differences between neutrophils treated with exRNaseA and those with mock treatment, for either resting neutrophils, or neutrophils activated *in vitro* or *in vivo* (Figures S1D–S1F). These data argue against that exRNaseA entered cells to digest intracellular RNAs. By contrast, the exRNaseA treatment substantially reduced glycoRNA signals from HOXB8 cells and HOXB8-differentiated neutrophils and nearly eliminated glycoRNA signals from PMNs (Figure 1C, right). To further test the localization of glycoRNAs on the outer cell surface, we labeled PMNs with Ac_4ManNAz and directly treated live cells with the hydrophilic click-chemistry substrate, DBCO-PEG₄-biotin, without permeabilizing the cells, then followed by RNA extraction and detection of biotin. This extracellular biotinylation of Ac_4ManNAz -labeled glycans yielded a strong signal in the RNA blot, which was completely abolished by exRNaseA digestion (Figure 1D). The data above are consistent with the notion that glycoRNAs are predominantly located on the outer cell surface of neutrophils.

To directly visualize RNA on neutrophil cell surface, we labeled cellular RNAs with the nucleoside homolog 5'-bromouridine (BrU) and detected cell surface RNAs by an anti-BrU antibody applied extracellularly on live neutrophils. Our initial attempts were unsuccessful, without detectable signals (see example in Figure 1E, 2nd row). We observed that cell surface glycoRNAs were at least 100-fold less sensitive to RNase A digestion than naked RNAs (Figure S1G), leading us to reason that cell surface RNAs may be protected by unknown proteins, which could block antibody's access to RNA. We therefore briefly pre-treated BrU-labeled live PMNs with a low concentration of Pro K before anti-BrU detection. We observed that Pro K digestion enabled the detection of BrU signals on cell surface, and these signals were sensitive to exRNaseA digestion (Figure 1E). Taken together, the data above support the existence of cell surface RNAs in neutrophils.

Cell surface RNAs control neutrophil recruitment to inflammatory sites *in vivo*

To determine whether cell surface RNAs control neutrophil functions *in vivo*, we utilized a thioglycolate (TG)-induced acute peritonitis model (Figure 2A), in which neutrophils are recruited to the peritoneum within hours. Specifically, mice were pre-treated

Figure 1. Detection of RNA on neutrophil surface

(A) HOXB8 cells or differentiated (Diff) HOXB8 cells were treated with or without Ac_4ManNAz . RNAs were extracted from the cells, and RNA samples were reacted with DBCO-PEG₄-biotin. RNAs were analyzed on an agarose gel (left) and then blotted with an anti-biotin antibody (right). Representative images are shown. (B) Bone marrow (BM) neutrophils were similarly labeled with Ac_4ManNAz and analyzed as in (A). After the click-chemistry reaction, RNAs were treated with RNase A in the presence or absence of RNase inhibitor or with Proteinase K (Pro K) or DNase I as indicated. Representative images are shown. (C) The indicated cell types were treated with or without Ac_4ManNAz . Cells were then treated extracellularly with RNase A (exRNaseA) or with mock treatment, washed, and then harvested for RNA. Analysis of RNA by gel and blotting was performed similarly as in (A). Representative images are shown. (D) BM neutrophils were treated with or without Ac_4ManNAz . Click-chemistry reaction with DBCO-PEG₄-biotin were performed directly on live cells without permeabilizing cell membrane. Cells were then treated with exRNaseA or mock conditions. RNAs were harvested and directly analyzed by gel and blotting without further click-chemistry reactions. Representative images are shown. (E) BM neutrophils were cultured with BrU for 24 h. Cells were further cultured for 30 min with Hoechst. Cells were then treated extracellularly with Proteinase K (exPro K) or with mock treatment and washed. Cells then underwent exRNaseA or mock treatment. Staining by a biotin-conjugated anti-BrU antibody and streptavidin was performed directly on live cells without permeabilizing the cell membrane. Representative images are shown. See also Figure S1.

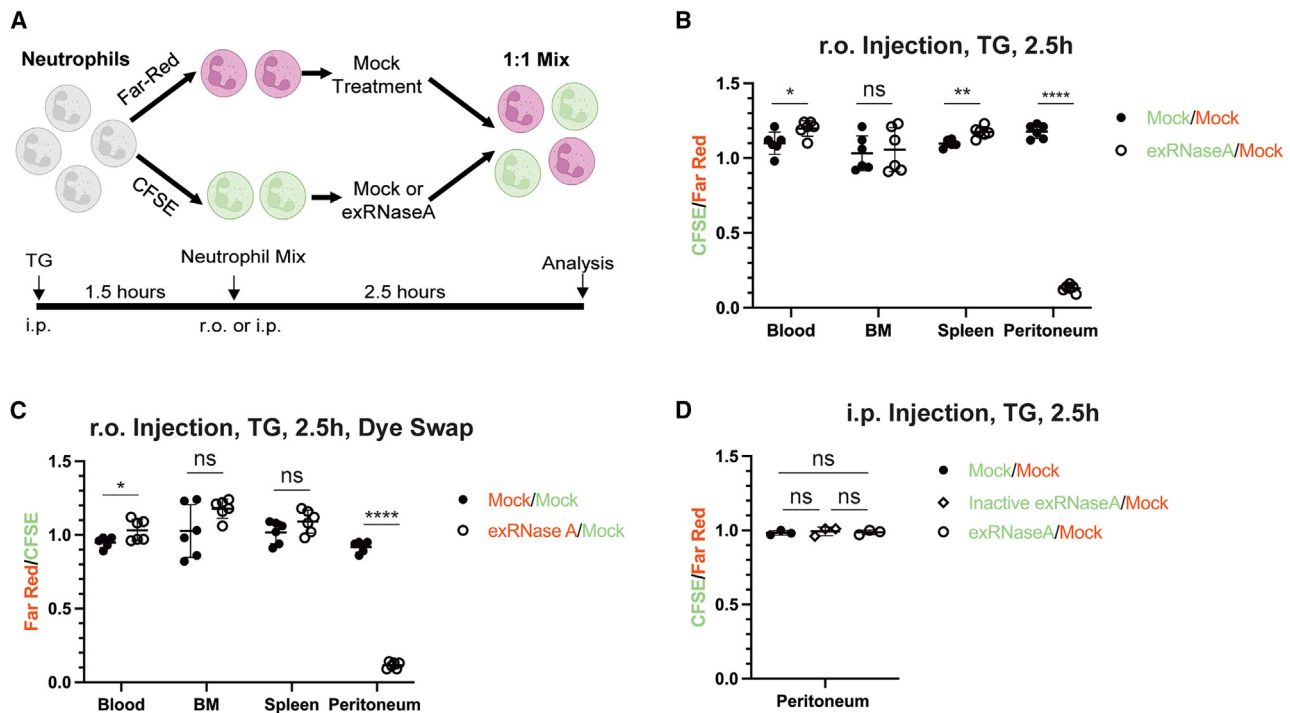


Figure 2. Ablating cell surface RNAs reduces neutrophil recruitment *in vivo*

(A and B) Bone marrow neutrophils were labeled with a green (CFSE) or a far-red dye. Cells then underwent mock or extracellular RNase A (exRNaseA) treatment before mixing test cells and control cells. Recipient mice were conditioned by intraperitoneal injection (i.p.) of thioglycolate (TG) 1.5 h prior to injecting the mixed neutrophils retro-orbitally (r.o.). Cells were harvested 2.5 h afterward from peripheral blood, bone marrow (BM), spleen, and peritoneum. (A) Schematics of the experiments. (B) Harvested cells were analyzed by flow cytometry, gating on Ly6G+ cells. The ratios between CFSE and far-red-labeled cells were plotted, with each dot representing a recipient mouse. $n = 6$. Data from a representative experiment are shown.

(C) A similarly experiment was performed as in (B), except that test cells were labeled by a far-red dye, whereas control cells were labeled with CFSE. $n = 6$. Data from a representative experiment are shown.

(D) A similar experiment was performed as in (B), except that the mixed neutrophils were directly injected into the peritoneal cavity. In addition, an experimental group of cells treated extracellularly with inactivated RNase A was included. $n = 3$. Data from a representative experiment are shown. For all panels, error bars represent standard deviation. * $p < 0.05$; ** $p < 0.01$; **** $p < 0.0001$; ns: not significant. See also Figure S2 and Table S1.

with TG, followed by injection of a mixture of neutrophils of two different colors into circulation, with the ratio between the two neutrophil populations assessed in the peritoneum after 2.5 h. PMNs were subjected to exRNaseA digestion. Mock-treated and exRNaseA-treated cells were then labeled with carboxy-fluorescein succinimidyl ester (CFSE, green) and far-red fluorescent pan-protein dyes, respectively, and mixed before injection. Compared with parallel experiments in which neither CFSE nor far-red neutrophils were treated with exRNaseA, we observed a ~9-fold reduction of neutrophils in the peritoneum after exRNaseA treatment (Figure 2B; Table S1). By contrast, exRNaseA-treated neutrophils were observed in peripheral blood, BM, and spleen at comparable or mildly elevated levels compared with the control group (Figure 2B), with the small increases likely secondary to the reduction of exRNaseA-treated neutrophils in the peritoneum. In comparison, treating cells with inactivated RNase A did not strongly affect the presence of peritoneal neutrophils (Figure S2A). A dye-swap experiment revealed a similar defect, where the exRNaseA-treated cells were labeled with the far-red dye and control cells with CFSE (Figure 2C). Of note, we verified that the recovery of glycoRNAs after exRNaseA treatment took much longer than the time frame

of this *in vivo* neutrophil assay (Figure S2C). The observed reduction of peritoneal neutrophils could be due to decreased recruitment of neutrophils to the peritoneum or decreased neutrophil viability after recruitment. Two lines of evidence argue against exRNaseA treatment reducing neutrophil viability. First, we observed similar viability of PMNs treated with exRNaseA and control cells for at least 10 h *in vitro* (Figure S2B). Second, we performed an experiment in which the neutrophils were injected directly into the peritoneum of TG-pre-conditioned mice and did not observe significant changes in the number of exRNaseA-treated neutrophils in the peritoneum compared with that of the controls (Figure 2D). When we extended the time from 2.5 to 6 h between neutrophil transfer into circulation and harvesting peritoneal cells, we again observed a strong decrease (~6-fold) of exRNaseA-treated neutrophils in TG-conditioned peritoneum (Figure S2D). To test whether this defect is restricted to TG-induced acute peritonitis, we used an acute lung inflammation model in which lipopolysaccharide (LPS) was introduced intranasally 16 h prior to retroorbital transfer of mock and exRNaseA-treated neutrophils. We observed a strong reduction of exRNaseA-treated neutrophil in the lung 2.5 h after the neutrophil transfer compared with mock-treated cells (Figure S2E), with

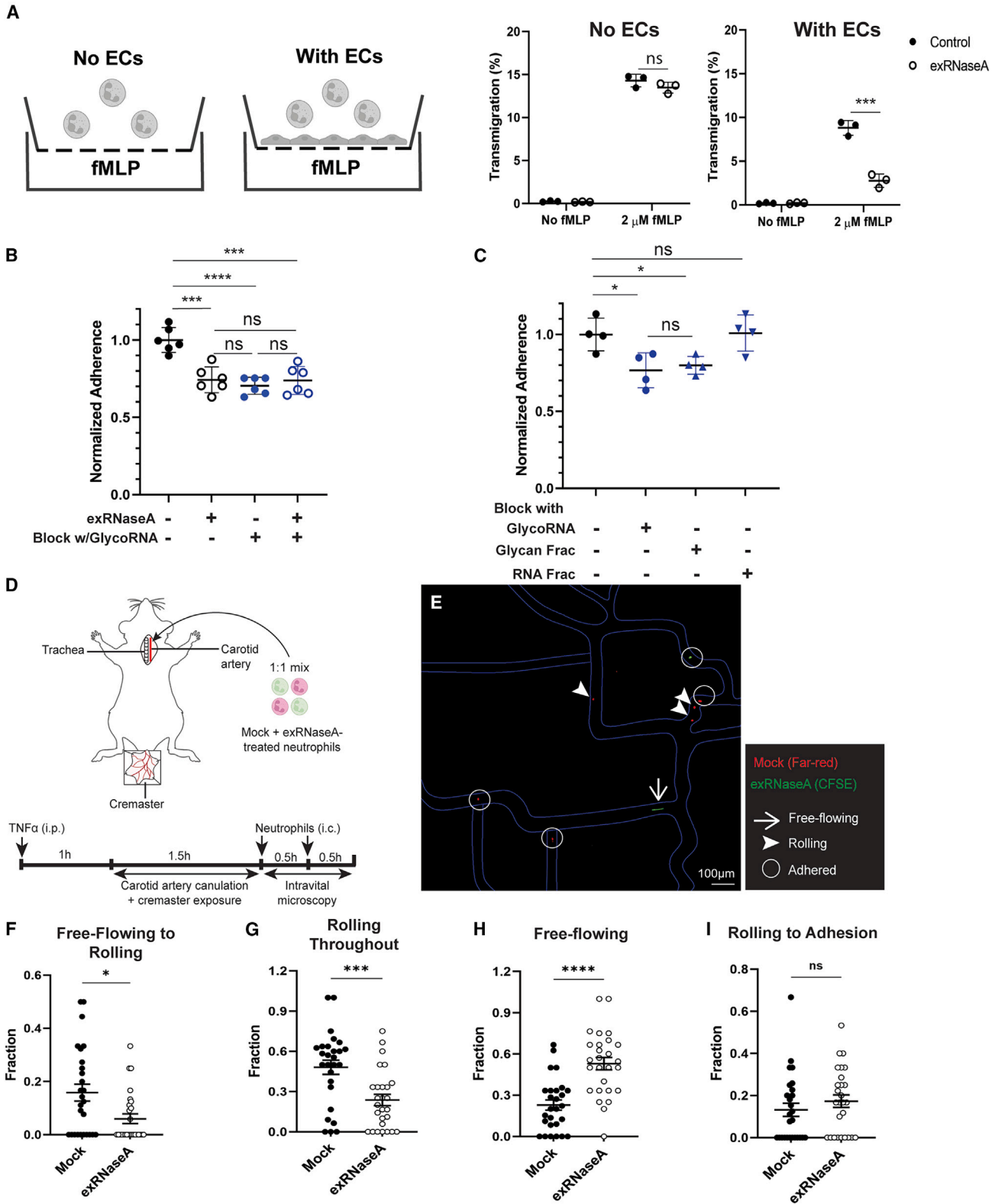


Figure 3. Ablating cell surface RNAs reduces neutrophil-endothelial cell interaction

(A) Bone marrow neutrophils underwent mock (control) or extracellular RNase A (exRNaseA) treatment. Cell migration was analyzed in a transwell assay with one group of experiments having endothelial cells (ECs) plated to cover the top surface of the transwell insert, whereas another group without ECs. For testing (legend continued on next page)

no or mild changes in peripheral blood, spleen, or BM. Taken together, the data above support that cell surface RNAs are required for efficient neutrophil recruitment to inflammatory sites *in vivo*.

Neutrophil glycoRNAs regulate vascular adhesion and transendothelial migration

Neutrophil recruitment from circulation to inflammatory sites *in vivo* involves complex cellular interactions and processes. To better understand the cellular functions of cell surface RNAs, we tested the functions of neutrophils *in vitro* to migrate across an endothelial layer toward a chemoattractant. We seeded murine endothelial cells (ECs) on top of a porous membrane in the upper chamber of a Boyden chamber and tested the migration of control or exRNaseA-treated neutrophils from the upper chamber toward N-formylmethionine-leucyl-phenylalanine (fMLP) signals in the bottom chamber. We observed a ~3-fold reduction in the migration of exRNaseA-treated neutrophils (Figure 3A). By contrast, no difference was observed in transwell migration in the absence of the endothelial layer (Figure 3A), indicating that cell surface RNAs do not directly affect neutrophils' ability to migrate in the absence of interaction with ECs. Of note, the levels of neutrophil glycoRNAs did not significantly change after migration (Figure S2F). The defect in transendothelial migration was partly due to reduced adhesion of neutrophils to the endothelial layer. We consistently observed a ~30% reduction of exRNaseA-treated neutrophils to adhere to ECs in the absence of liquid flow (Figure 3B), which was further affected in the presence of 2 dynes/cm² of flow shear force to mimic circulation (Figure S3A). These data support that cell surface RNAs are necessary for efficient neutrophil-endothelial interactions. Of note, ECs contain weak or no glycoRNA signals themselves when labeled with Ac₄ManNAz (Figure S3B). To address whether the defective adhesion and transendothelial migration of exRNaseA-treated neutrophils is contributed by the lack of glycoRNAs, we blocked ECs with a saturating level of glycoRNAs isolated from neutrophils (Figure S3C) before assessing the adhesion of neutrophils. Blocking ECs with purified glycoRNAs

was sufficient to reduce the adhesion of untreated neutrophils to a similar level as that of exRNaseA-treated neutrophils without endothelial blockage (Figures 3B and S3C). Combining both exRNaseA treatment of neutrophils and blocking ECs with glycoRNAs did not further reduce cell adhesion (Figure 3B), therefore supporting a model in which glycoRNAs underlie the cell-surface-RNA-mediated adhesion of neutrophils to ECs. To determine whether it is the RNA fraction or the glycan fraction that mediates the function of glycoRNAs, we used Peptide:N-glycosidase F (PNGase F), previously reported to release the glycan from glycoRNAs.² We confirmed that the glycoRNA signals based on the Ac₄ManNAz tracer were abolished by PNGase F treatment (Figure S3D). Using PNGase F, we separated the RNA and glycan fractions from purified neutrophil glycoRNAs and blocked ECs with them separately. Blocking with the glycan fraction effectively reduced neutrophil adhesion to and migration through an endothelial layer to similar levels as blocking with glycoRNAs, whereas blocking with the RNA fraction did not change neutrophil-endothelial adhesion or transendothelial migration (Figures 3C and S3E). Taken together, the data above support that neutrophil cell surface RNAs play an important role in neutrophil interaction with ECs, with the functions of the cell surface RNAs attributable to the glycans on glycoRNAs.

To examine the importance of cell surface RNAs in neutrophil-endothelial interaction *in vivo*, we performed intravital imaging. Mock-treated and exRNaseA-treated neutrophils were labeled with green and red dyes separately (with dye swapping in different experiments), then 1:1 mixed and injected into the carotid artery of mice preconditioned with tumor necrosis factor alpha (TNF- α). Dye-labeled neutrophils passing through the blood vessels at the cremaster region and their interaction with the endothelium were imaged and quantified (Figure 3D). For each blood vessel under imaging, we quantified the fraction of neutrophils from each group that transitioned from free flowing to rolling on the endothelium, the fraction that kept rolling throughout the imaging interval, and the fraction transitioning from rolling to stable adhesion. We observed that the exRNaseA treatment led to significant decreases of the fractions of

migration, neutrophils were added to the top chamber with the chemoattractant fMLP (2 μ M) added to the bottom chamber. Left: schematics for experiments. Right: the numbers of the migrated cells were quantified and normalized as percentages of input cells. Each dot represents a biological replicate. $n = 3$. Data from representative experiments are shown.

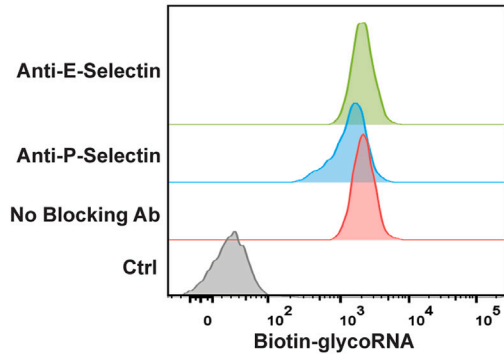
(B) The static adhesion of bone marrow neutrophils to ECs was analyzed, where ECs were pre-plated as a confluent layer in culture dishes. Neutrophils were dye-labeled (to facilitate counting on ECs) and treated with or without exRNaseA. In the indicated conditions, glycoRNAs purified from neutrophils were used to pre-block the ECs. For assaying adhesion, neutrophils were added to EC-plated dishes for 10 min, followed by washes to remove unattached or loosely attached neutrophils. Cells were then counted under microscope, with adherence quantified as the number of neutrophils averaged across at least 10 random imaging fields, and normalized to the control (no exRNaseA, no glycoRNA blocking) group. Each dot represents a biological replicate. $n = 6$. Data from a representative experiment are shown.

(C) A similar experiment as in (B) was performed, except that in addition to blocking ECs with glycoRNAs, blocking with the glycan fraction and the RNA fraction of the neutrophil glycoRNAs was performed. $n = 4$. Data from a representative experiment are shown.

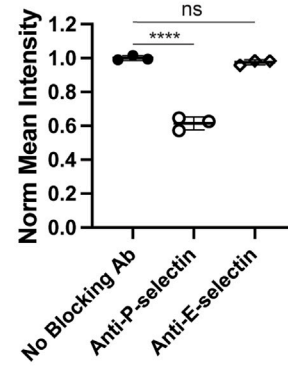
(D–I) Intravital imaging experiments were performed to assay differential neutrophil-endothelial interactions by mock and exRNaseA-treated neutrophils *in vivo*.

(D) The schematics of the experiment. A 1:1 mixture of mock and exRNaseA-treated neutrophils was administered via intracarotid (i.c.) injection to C57BL/6 mice previously stimulated with TNF- α . Intravital confocal microscopy was performed to analyze rolling and adhesion of injected neutrophils to the blood vessels of the cremaster muscle. exRNaseA- or mock-treated neutrophils were labeled with CFSE or far-red cell tracer. Two independent experiments for each labeling combination were carried out. (E) A representative confocal image of the cremaster microcirculation, with blood vessel linings indicated by blue lines, with different states of neutrophils indicated by symbols in the legend. (F–I) The numbers of neutrophils that were free rolling, transitioned from free rolling to rolling, kept rolling throughout the imaging interval, or transitioned from rolling to stable adhesion were quantified. Data were normalized to reflect the fractions of neutrophils within a given color that display the corresponding behavior in a field. Each dot represents data from a field at one of the imaging intervals. For all panels, except for (F)–(I), error bars represent standard deviations. For (F)–(I), error bars represent SEM. * $p < 0.05$; *** $p < 0.001$; **** $p < 0.0001$; ns: not significant. See also Figure S3 and Video S1.

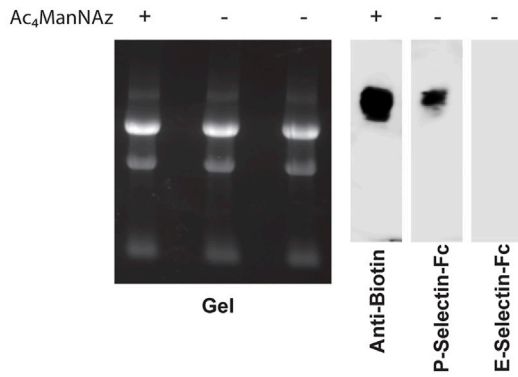
A Blocking ECs with anti-Selectin Ab



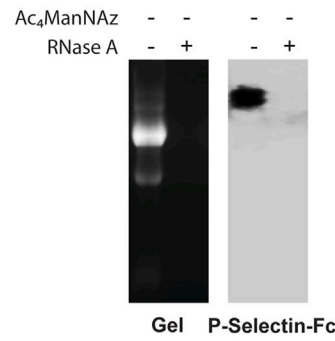
B



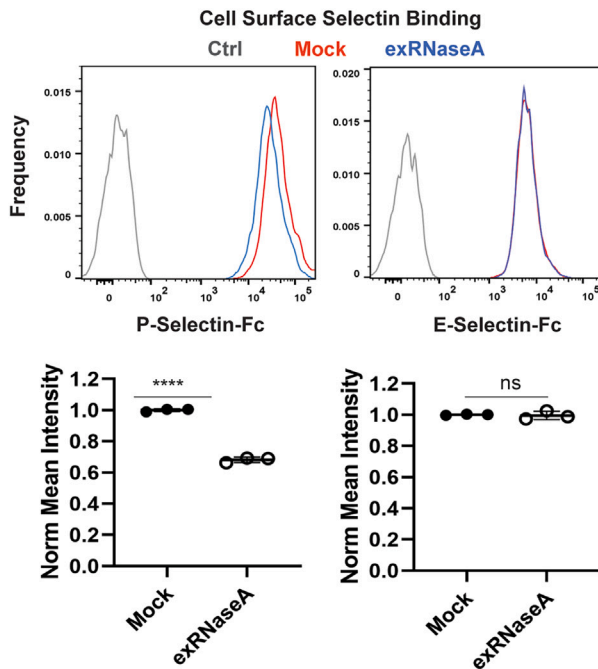
C



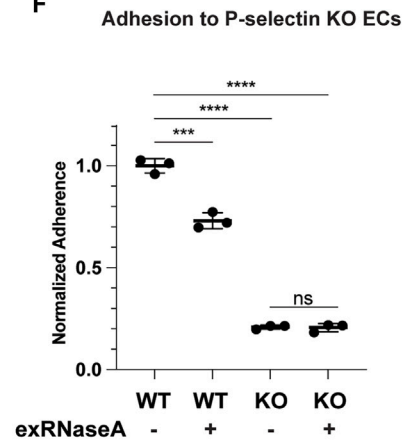
D



E



F



(legend on next page)

neutrophils transitioning from free flowing to rolling as well as those rolling throughout (Figures 3E–3G; Video S1). Consistently, there was a concomitant increase of the fraction of free-flowing neutrophils in the exRNaseA-treated group (Figure 3H). The fraction of neutrophils transitioning from rolling to stable adhesion was not significantly different (Figure 3I). These data suggest a role of cell surface RNAs in regulating the initial capture and rolling of neutrophils on the vascular wall *in vivo*.

Neutrophil glycoRNAs can be recognized by endothelial Selp

Integrins and lectin ligands on neutrophils are known to have important roles in the neutrophil-endothelial interactions.⁸ We first investigated if neutrophil cell surface RNAs regulate neutrophil integrin abundance or activity. Removal of neutrophil surface RNAs with exRNaseA treatment did not significantly change cell surface levels of integrins Cd11a and Cd11b (Figure S4A) or neutrophil interaction with the integrin ligand intercellular adhesion molecule 1 (ICAM-1, Figure S4B). Neutrophil spreading on fibrinogen-coated surfaces was also unchanged with exRNaseA treatment (Figure S4C). P-selectin (Selp) and E-selectin (Sele) are the main lectins known to be expressed in ECs that translocate to EC membrane upon proinflammatory signals to recognize sialic-acid-containing ligands.⁹ Selp is required for the early stage of neutrophil recruitment after TG-induced peritoneal inflammation,^{10,11} and both Selp and Sele play a redundant role during later stages of neutrophil recruitment.¹¹ Siglec receptors, also capable of binding sialic-acid-containing ligands, are expressed at low or non-detectable levels in public mouse EC RNA-seq data (Figure S4D). To determine whether Selp or Sele are involved in interaction with glycoRNAs, we first treated ECs with purified biotin-labeled glycoRNAs followed by flow cytometry using fluorescently labeled streptavidin, yielding positive signals (Figure 4A), indicating that glycoRNAs can directly bind to the EC surface. When ECs were pre-treated with a blocking antibody against Selp, we observed a significant reduction in glycoRNA binding (Figures 4A and 4B), whereas glycoRNA binding was not affected by a blocking antibody against Sele (Figures 4A and 4B). To further confirm the role of Selp, we knocked out Selp in ECs via CRISPR (Figure S4E) and observed a ~3-fold reduction of glycoRNA binding to EC surface (Figure S4F). To determine whether Selp could directly interact

with RNA ligands, we ran RNAs from neutrophils on an RNA gel and blotted with a recombinant Selp-Fc fusion protein. Detection by Selp-Fc yielded positive signals, whereas no signal was detected by a recombinant Sele-Fc fusion protein (Figure 4C). The electrophoretic mobility of Selp-Fc-detected signals was within the range detected for biotin-labeled glycoRNAs (Figure 4C) but appeared with a narrower mobility distribution, suggesting that Selp may interact with a fraction of neutrophil glycoRNAs. The Selp-Fc detected signals were abolished when purified neutrophil RNA was digested with RNase A (Figure 4D), confirming that Selp-Fc recognizes RNA-containing ligands. We reasoned that if neutrophil cell surface glycoRNAs represented a significant source of Selp ligands, treating live neutrophils with exRNaseA would reduce cell surface Selp-Fc binding. Indeed, we observed a ~30% reduction by flow cytometry (Figure 4E), similar to the level of reduced neutrophil adhesion to ECs after exRNaseA treatment. The remaining Selp binding signals are likely contributed by other Selp ligands. By contrast, exRNaseA treatment did not affect Sele-Fc binding to neutrophil surface (Figure 4E). The level of cell surface PSGL-1 (Selpig), a glycoprotein in neutrophils and a known ligand for Selp and other selectins,^{12,13} was not affected by exRNaseA treatment (Figure S4G), nor was the level of neutrophil cell surface L-selectin (Figure S4H). To determine whether neutrophil cell surface RNAs facilitate neutrophil adhesion to ECs via Selp, we quantified the adhesion of mock and exRNaseA-treated neutrophils to wild-type (WT) and Selp-knockout (KO) ECs. Consistent with the importance of Selp, Selp KO ECs substantially reduced neutrophil adhesion, but exRNaseA treatment of neutrophils did not further reduce adhesion (Figure 4F). Our intravital imaging results (Figures 3D–3I) are also consistent with endothelial Selp being a receptor for neutrophil glycoRNAs since Selp is known to regulate the initial capture and rolling of neutrophils on vessel walls.^{14,15} Taken together, these data support that neutrophil glycoRNAs can be recognized by Selp on ECs to facilitate neutrophil-endothelial interaction.

SIDT family genes are required for neutrophil glycoRNAs

There are two models that may explain the presence of RNAs on neutrophil cell surface. In the first model, cellular RNAs are released from one cell, such as via membrane breakage, and then captured by another cell on the cell surface. In the second

Figure 4. Neutrophilic glycoRNAs interact with Selp

(A) Endothelial cells (ECs) were blocked with anti-Selp or anti-Sele antibodies before biotin-labeled glycoRNAs were added to assay binding to ECs. GlycoRNAs were purified from Ac₄ManNAz-treated bone marrow neutrophils and labeled with biotin through click chemistry. ECs were dissociated by an enzyme-free buffer, and the levels of glycoRNA binding were quantified using flow cytometry via streptavidin. ECs analyzed without streptavidin (Ctrl) or without antibody blocking were used as controls. Representative flow cytometry plots are shown.

(B) Data in (A) were quantified as mean fluorescence intensity, normalized by the control condition without blocking antibody. Each dot represents a biological replicate. n = 3. Data from a representative experiment are shown.

(C) RNAs were harvested from bone marrow neutrophils treated with or without Ac₄ManNAz. RNAs from cells with Ac₄ManNAz were labeled with biotin through click chemistry. RNAs were analyzed by gel and were blotted with anti-biotin, or with recombinant proteins of Selp-Fc fusion or Sele-Fc fusion. Representative images are shown.

(D) A similar experiment as in (C) was performed, including a condition with purified RNAs treated with RNase A before gel and blot analysis.

(E) Bone marrow (BM) neutrophils underwent exRNaseA or mock treatment. Recombinant Selp-Fc or Sele-Fc were used to bind to live neutrophils. Top: representative flow cytometry plots showing the levels of Selp and Sele binding signals, with unstained cells as negative control (Ctrl). Bottom: quantified mean fluorescence intensity was normalized by the mock treatment condition. n = 3. Data from a representative experiment are shown.

(F) BM neutrophils were treated with mock or exRNaseA and subjected to *in vitro* adhesion assay to WT and Selp KO ECs. n = 3. Data from a representative experiment are shown. For all panels, error bars represent standard deviation. ***p < 0.001; ****p < 0.0001; ns: not significant. See also Figure S4.

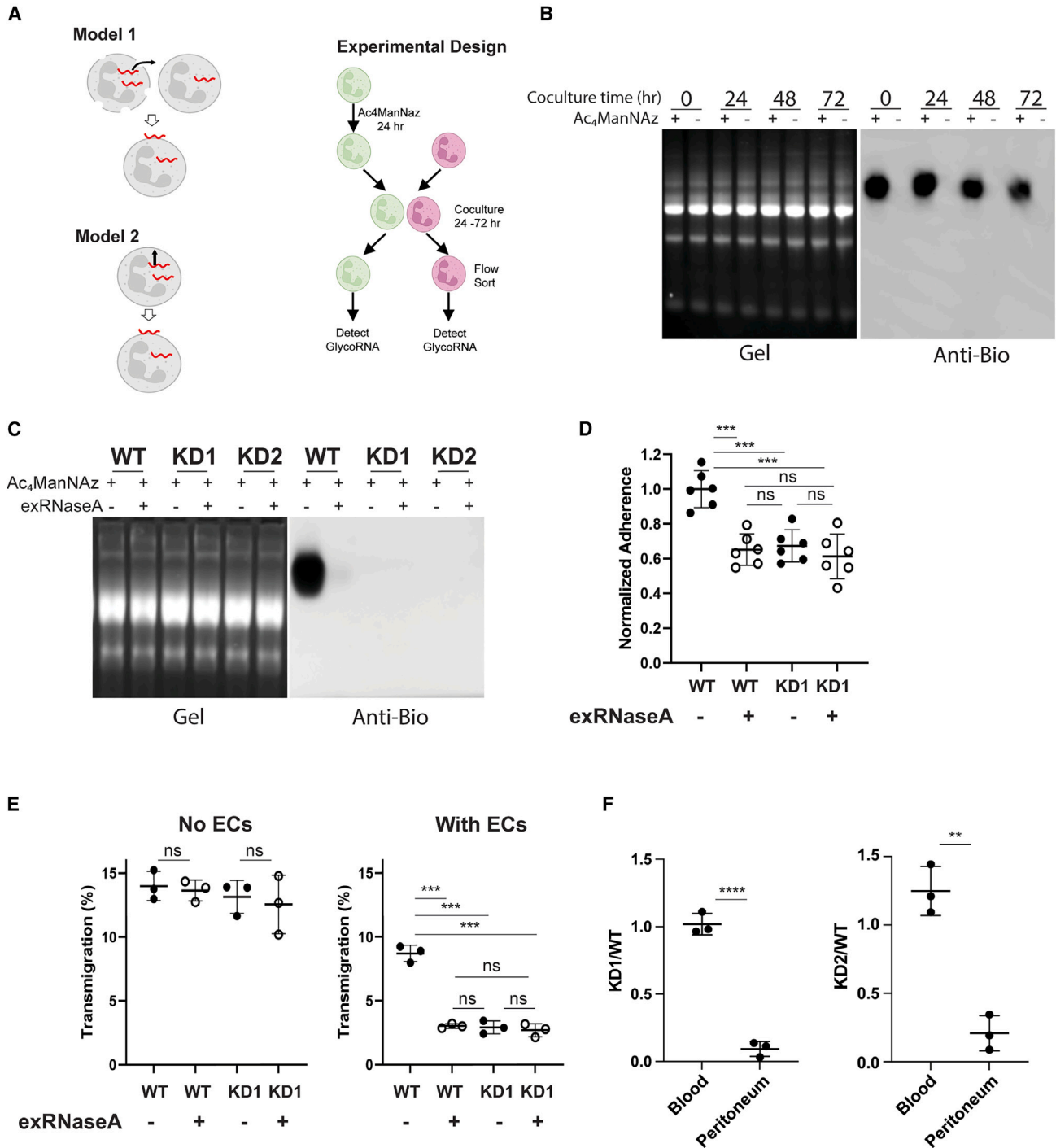


Figure 5. *Sidt* family transporters are required for glycoRNA production and neutrophil-endothelial cell interaction

(A) Model 1 depicts that RNA (red) molecules are released from originating cells and captured by other cells. Model 2 depicts cell-intrinsic production and transfer of RNA to cell surface. Experiments were designed to distinguish the two models via the schematics on the right. BM neutrophils were treated with or without Ac₄ManNAz for 24 h, with Ac₄ManNAz-treated cells labeled with a green dye and untreated cells with a red dye. Cells were mixed together and co-cultured for 24–72 h before FACS to isolate live green and red cells. RNAs were harvested from the sorted cell populations and analyzed by gel and blotted for glycoRNA similar to experiments in Figure 1A.

(B) Data for the experiment in (A), with representative images shown.

(legend continued on next page)

model, cellular RNAs are produced and transported to the cell surface in the same cell. To determine which of these two models apply to the presence of glycoRNAs on cell surface, we performed a co-culture experiment. One group of neutrophils was labeled with Ac₄ManNAz for 1 day followed by labeling with a green dye (CFSE) and extensive washes to remove any extra Ac₄ManNAz. Another group of neutrophils was labeled with a red dye without Ac₄ManNAz labeling. These cells were then mixed and co-cultured for one to 3 days before fluorescence-activated cell sorting (FACS) into live green and red cells (Figure 5A). Model 1 predicts that Ac₄ManNAz-labeled glycoRNAs should be detected in both green and red cells, whereas model 2 predicts the presence of Ac₄ManNAz-labeled glycoRNAs in green cells only. We observed strong signals from Ac₄ManNAz-labeled glycoRNAs in green cells but not red cells (Figure 5B). Given that glycoRNAs are primarily located on the cell surface of neutrophils, these data support that glycoRNAs are produced and transported to cell surface in a cell autonomous manner.

Topologically, transportation of intracellular RNA to the outer cell surface requires RNAs to cross membrane at least once. The mammalian *Sid1* and *Sid2* genes, homologs of the *Caenorhabditis elegans sid-1* RNA transporter,^{16,17} have been shown to facilitate the transport of RNAs across cellular or intracellular vesicle membranes.^{18–21} Both *Sid1* and *Sid2* are expressed in murine neutrophils (Figure S5A) and HOXB8 cells (Figure S5B). To determine the role of *Sid1* genes in glycoRNA production, we used two independent multi-sgRNA vectors, each knocking down (KD) both *Sid1* and *Sid2* in HOXB8 cells with high KD efficiencies (Figure S5B). Strikingly, Ac₄ManNAz-labeled glycoRNAs were abolished in *Sid1*-KD cells (Figure 5C), whereas Ac₄ManNAz labeling of other cell surface components was unaffected (Figure S5C). These data indicate that *Sid1* RNA transporters are required for the presence of sialic-acid-containing glycoRNAs in cells. We next tested whether the functions of cell surface RNAs depend on *Sid1*. Similar to PMNs, exRNaseA treatment reduced the transendothelial migration by HOXB8-differentiated neutrophils by ~3-fold, without affecting migration in the absence of ECs (Figures 5E and S5E). Differentiated neutrophils from *Sid1*-KD HOXB8 cells showed a similar level of reduction in transendothelial migration (Figures 5E and S5E). Importantly, exRNaseA treatment did not further inhibit the transendothelial migration of the *Sid1*-KD cells (Figures 5E and S5E). Similarly, *Sid1*-KD reduced the adhesion of HOXB8-differentiated neutrophils to ECs by ~30%–40%, a level similar to exRNaseA-treated control cells, and exRNaseA treatment did not further exacerbate the KD phenotype (Figures 5D and

S5D). To determine whether *Sid1*-KD affects neutrophil recruitment *in vivo*, we mixed WT and *Sid1*-KD HOXB8-derived neutrophils that were differentially dye-labeled and quantified their migration to the peritoneum in the TG-induced acute peritonitis model. We observed a >5-fold reduction of *Sid1*-KD neutrophils in the peritoneum when compared with the WT neutrophils (Figure 5F), similar to the effect of removing neutrophil cell surface RNAs (Figure 2). Taken together, the data above indicate that *Sid1* genes are required for both glycoRNAs and cell surface RNA functions in neutrophils.

Neutrophil glycoRNAs are predominantly small RNAs mappable to noncoding transcripts

To characterize the types of RNAs that constitute neutrophil glycoRNAs, we used two strategies to purify glycoRNAs from total RNAs. In the first method, we subjected total RNAs from Ac₄ManNAz-labeled HOXB8-derived neutrophils to purification by streptavidin-based pull-down of biotin-labeled glycoRNAs. In the second method, total RNAs from both PMNs and HOXB8-derived neutrophils (without Ac₄ManNAz labeling) were purified by affinity to the lectin wheat germ agglutinin (WGA). Purified glycoRNAs were devoid of major rRNA bands and showed a smearing pattern on Bioanalyzer (Figure 6A). Removing glycans by PNGase F digestion resulted in the purified RNAs appearing primarily in the small RNA range (Figure 6A). These results are consistent with the report of glycoRNAs being small RNAs in cell lines² and that the relatively slow mobility of glycoRNAs on RNA gels or the Bioanalyzer matrix are likely due to glycans affecting the mobility of RNAs. We prepared small RNA-seq libraries and sequenced the purified glycoRNAs from PMNs, HOXB8 cells, and HOXB8-differentiated neutrophils (Figure 6B). We also prepared libraries for input controls, which were generated from purified small RNA fractions of the corresponding input total RNA. Analysis of sequencing reads showed that WGA and biotin purifications yielded similar small RNA profiles (Figure S6A), suggesting that both WGA and biotin purifications had low backgrounds since these two purification methods used different principles and affinity reagents, and further arguing against the existence of major artifacts of the Ac₄ManNAz-DBCO-biotin labeling strategy. Removal of glycans by PNGase F digestion before library preparation also did not substantially change the small RNA profile (Figure S6B). Most of the small RNAs were mapped as fragments of noncoding RNA species from the nuclear genome, such as rRNAs, tRNAs, and small nucleolar RNAs (snoRNAs) (Figure S6C). Comparing our murine neutrophil data to glycoRNA sequencing results of human H9 and HeLa cells from Flynn et al.,² we noticed that sequence

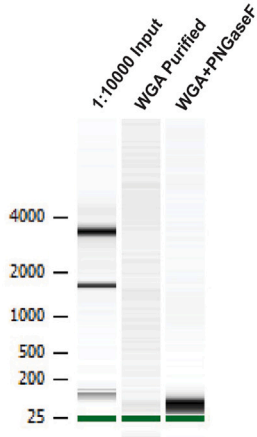
(C) Cas9-expressing HOXB8 cells were transduced with a control sgRNA (wild type or WT) or two independent sets of sgRNAs to knock down (KD) the expression of *Sid1* and *Sid2*. Cells were differentiated toward neutrophils and treated with Ac₄ManNAz. Cells were further subjected to exRNaseA or mock treatment. RNAs were harvested and subjected to analysis of glycoRNA via gel and immunoblotting. Representative images are shown.

(D) Neutrophils differentiated from WT and *Sid1*-KD HOXB8 cells were subjected to exRNaseA or mock treatment. Cells were analyzed for adhesion to endothelial cells (ECs) similar to Figure 3B. Each dot represents a biological replicate. *n* = 6. Data from a representative experiment are shown.

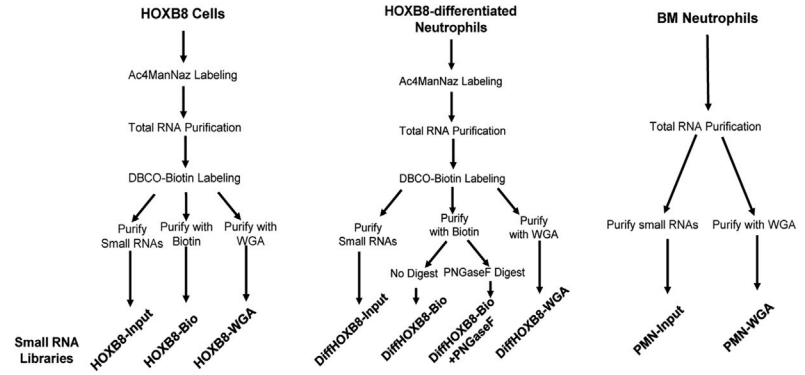
(E) Cells in (D) were analyzed for transmigration with or without ECs, similar to experiments in Figure 3A. Each dot represents a biological replicate. *n* = 3. Data from a representative experiment are shown.

(F) WT and *Sid1*-KD HOXB8 cells were differentiated *in vivo* to obtain WT and *Sid1*-KD neutrophils. These neutrophils were dye-labeled, mixed, and injected into recipient mice to assay for recruitment to the peritoneum in the acute peritonitis model in Figure 2A. Ratios of KD to WT cells were quantified in the indicated tissues, with data from two independent sgRNA KD vectors. *n* = 3. Data from representative experiments are shown. For all panels, error bars represent standard deviation. ***p* < 0.01; ****p* < 0.001; *****p* < 0.0001; ns: not significant. See also Figure S5.

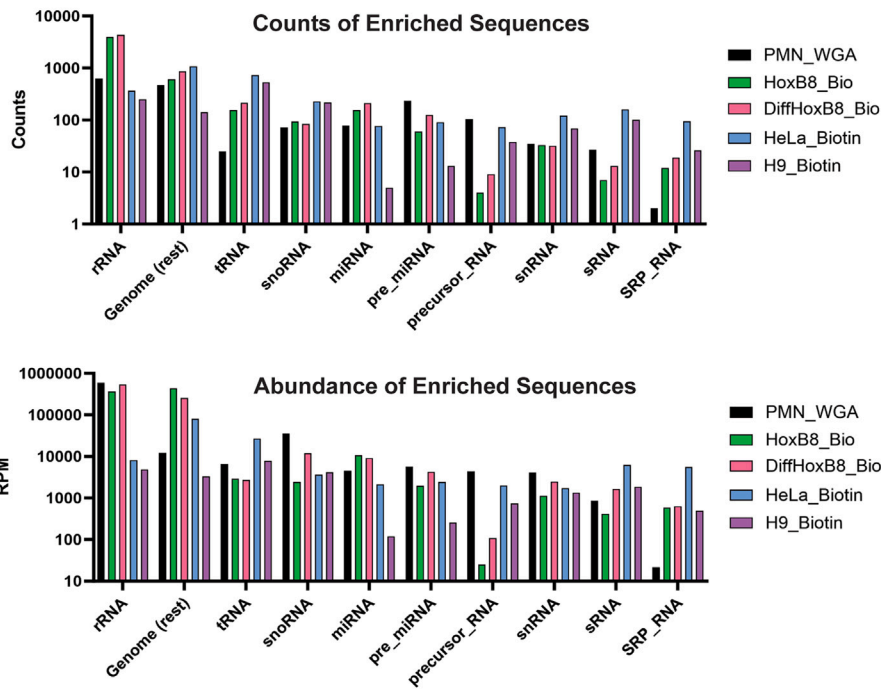
A



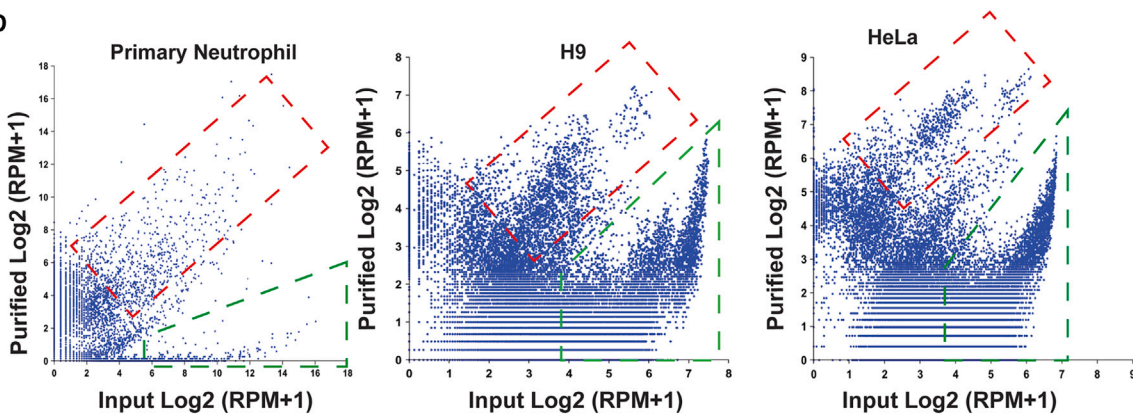
B



C



D



(legend on next page)

reads were mapped to similar classes of RNAs between the datasets (Figure S6C), with the exception that reads mappable to Y RNAs were present at low levels in both the input and glycoRNA fractions from murine neutrophils. On the level of each individual sequence, we observed many sequences were enriched in the glycoRNA fractions compared with the input samples (Figures 6C and 6D; Table S2), with most of the enriched sequences mappable to known classes of noncoding RNAs (Figure 6C). On the level of exact sequence isoforms, we did not identify any enriched glycoRNA sequence that was shared between our murine neutrophil data and those from the two human cell lines. Nevertheless, when we plotted the sequence abundances of the glycoRNA fraction versus those of the input, we noticed a shared feature among these datasets. The sequences could be separated into a group that was more enriched in the glycoRNA fraction (Figure 6D, red dashed boxes), with the levels of these enriched glycoRNAs showing correlation with their abundance in the input. By contrast, there was also a clearly separable group of sequences that were more depleted (Figure 6D, green dashed boxes) and sometimes a distinct third group in between. These data suggest that glycoRNAs originate from the most abundant small RNAs in the cell, with a yet-to-be-identified mechanism to either license certain cellular small RNAs to become glycosylated, or gate out certain RNAs from glycosylation, or both. In the case of enriched glycoRNA sequences in primary murine neutrophils, we noticed that a small number of sequences dominated the glycoRNA libraries, and they were mappable to abundant noncoding RNAs (Figure S6D). For example, two isoforms of a small RNA mappable to the 5' end of 45S pre-rRNA accounted for >25% of the reads in the glycoRNA library from neutrophils (Figure S6E; Table S2), which we validated by RT-qPCR (Figure S6F). These two sequences were also abundant in the glycoRNA fractions from HOXB8 cells and HOXB8-derived neutrophils (Figure S6E). These data support that glycoRNAs in neutrophils are predominantly small RNAs derived from abundant noncoding transcripts.

DISCUSSION

In this study, we demonstrate that cell surface RNAs play a critical role in neutrophil recruitment *in vivo*. This effect could be partly explained by cell surface RNAs controlling neutrophil adhesion to ECs and transendothelial migration *in vitro*, with both primarily contributed by the glycans of neutrophil glycoRNAs. We further demonstrate that the lectin Selp, but not Sele, can recognize at least a subset of neutrophil glycoRNAs. It is well appreciated that Selp recognizes ligands with sialic

acid moieties and has strong binding selectivity among sialic-acid-containing glycoproteins.^{12,22,23} Only a small number of glycoproteins²⁴ or glycolipids²⁵ have been implicated as the ligands for Selp, among which PSGL-1 has been best characterized and demonstrated as a functional Selp ligand *in vivo*.²⁶ However, PSGL-1 can be recognized by Sele as well.^{12,13} Our findings not only establish RNA-based ligands for Selp but also raise the interesting possibility that glycoRNAs could provide ligand specificity to even highly similar lectin proteins.

We also found that glycoRNAs are surprisingly stable, despite being primarily on the outer cell surface of neutrophils, as evidenced by their low rates of turnover in the glycoRNA recovery experiment and in the label-chase experiment (Figures 5B and S2C). We estimate from these experiments that the average half-life of neutrophil glycoRNAs is on the order of 24 h or more. Our observations further suggest that the RNA portion of cell surface glycoRNAs is heavily protected against RNase accessibility, likely by yet-to-be-identified protein(s) on cell surface, whereas the glycan portion is exposed and can be bound by P-selection. This protection model is consistent with our observation that the glycan fraction, rather than the RNA fraction, accounts for cell surface RNAs' function in mediating neutrophils' adhesion to and migration through an endothelial layer. This model could also explain the puzzle of why RNAs can be located on the outer cell membrane without being easily degraded. Future studies could further investigate this model. Our data support that glycoRNAs are produced and translocated to cell surface in a cell autonomous manner. Although the production of glycoRNAs requires several glycosylation enzymes important for protein N-glycosylation,² our findings of the role of the *Sidt* RNA transporters in regulating glycoRNA levels provide an RNA-specific link. Both *Sidt1* and *Sidt2* have been described to be present on the membranes of intracellular organelles,^{20,27,28} which may facilitate RNAs to enter such organelles to be glycosylated.

Limitations of the study

As the cell surface RNA/glycoRNA field is at its infancy, many exciting questions would require future explorations to address, such as the chemical nature of glycoRNAs, the mechanisms of their biogenesis, protection, and anchoring, rules governing cellular RNAs to become glycosylated, and their regulation/dysregulation in physiologic and disease conditions. It is also unclear whether the previously reported maxRNAs¹ are glycosylated or not, and our data do not exclude the possibility that there are non-glycosylated cell surface RNAs playing functional roles in neutrophils or other cell types.

Figure 6. Murine neutrophil glycoRNAs are primarily small RNAs from noncoding transcripts

(A) Total RNAs from BM neutrophils (input) were purified for glycoRNAs by WGA beads. The purified glycoRNA fraction was digested with PNGase F. The sizes of RNAs were analyzed on a Bioanalyzer with a broad range high sensitivity RNA analysis cartridge. Numbers indicate lengths of nucleotides. Of note, the exact sizes of small RNAs may not be fully accurate on this analysis platform.

(B) Purification and processing schemes for small RNA library preparation. HOXB8 cells, HOXB8-derived neutrophils, and BM neutrophils were used.

(C) Top: sequences enriched in the glycoRNA fractions from the indicated samples were counted and categorized based on the types of RNAs that they mapped to. Bottom: the total abundance of enriched glycoRNA sequences that mapped to the indicated RNA categories was calculated for each of the samples. RPM, reads per million mapped reads.

(D) The levels of RNA sequences in purified glycoRNA samples were plotted against those of the input samples, with the cell types indicated at the top. The red dashed boxes indicate sequences that are more enriched and show positive correlation to input sequence abundance, whereas the green dashed boxes indicate sequences that are depleted from the purified glycoRNA samples. See also Figure S6 and Table S2.

The current technologies for detecting glycoRNAs require substantial numbers of cells. This limitation makes it difficult to examine glycoRNA levels on subsets of neutrophils, such as those undergoing aging or in different maturation or activation states. We noticed a recent study using proximity ligation to image glycoRNAs in single cells based on the principle of the close proximity between sialic acid and a candidate glycoRNA sequence.²⁹ This technology may provide a strategy for examining glycoRNAs in small subsets of neutrophils but will require further refinements to exclude signals that arise from separate RNA and sialic acid molecules that are in close proximity.

Our data showed that the removal of cell surface RNAs strongly impaired (~9- to 10-fold reduction) neutrophil recruitment to inflammatory sites in two independent acute inflammation models *in vivo*, yet the effect size on neutrophil-endothelial adhesion *in vitro* is weaker (~30% reduction in static adhesion assays). One possible explanation of this discrepancy is that for neutrophils to be recruited to the right place *in vivo*, the cells need to undergo multiple steps of cell-cell interaction. If more than one step of cell-cell interactions is impaired, it can lead to a stronger overall difference. Second, we observed larger effect sizes under liquid flow conditions both *in vitro* and *in vivo*. Third, our data support that cell surface RNAs control the efficiency of neutrophils to migrate through an endothelial layer, the effect size of which is larger than that for the neutrophil-endothelial adhesion alone. Although this function in transendothelial migration cannot be easily explained by known functions of Selp, our data do suggest that Selp is not the only receptor for neutrophil glycoRNAs. Future work could explore additional receptors for neutrophil glycoRNAs and their functions.

Given that glycoRNAs can be found in many cell types,² which is corroborated by our unpublished observations, we speculate that glycoRNAs could play important functions across multiple cell types and in multiple biological settings.

STAR★METHODS

Detailed methods are provided in the online version of this paper and include the following:

- KEY RESOURCES TABLE
- RESOURCE AVAILABILITY
 - Lead contact
 - Materials availability
 - Data and code availability
- EXPERIMENTAL MODEL AND STUDY PARTICIPANT DETAILS
 - Mice
 - Cell culture
- METHOD DETAILS
 - Plasmids
 - Generating KO or KD cells
 - Neutrophil isolation from bone marrow
 - May-Grunwald-Giemsa staining
 - Ac₄ManNAz treatment
 - RNA extraction and purification
 - Enzymatic treatment of RNA samples and cells
 - Copper-free click chemistry reaction

- RNA gel electrophoresis, blotting, and imaging
- Imaging of cell surface RNAs
- Analysis of neutrophil recruitment *in vivo*
- Analysis of neutrophil plasma membrane integrity
- Neutrophil transwell migration *in vitro*
- Analysis of neutrophil cell surface integrins, PSGL-1 and L-selectin
- Neutrophil spreading assay
- Analysis of neutrophil adhesion on ECs
- Intravital confocal microscopy
- Label-based and label-free purification of GlycoRNAs
- RNA and glycan fraction preparation from glycoRNAs
- Flow cytometry
- Testing whether glycoRNAs were produced in a cell-intrinsic manner
- Western blot analysis
- RT-qPCR
- RNAseq analysis
- GlycoRNA sequencing
- QUANTIFICATION AND STATISTICAL ANALYSIS
 - Sequencing data analysis
 - Statistics

SUPPLEMENTAL INFORMATION

Supplemental information can be found online at <https://doi.org/10.1016/j.cell.2023.12.033>.

ACKNOWLEDGMENTS

We thank David Sykes for providing the Hoxb8-ER vector. We thank Qinrong Wang for the initial evaluation of the Hoxb8-based immortalization protocol and Yan Zeng for providing reagents for Selp KO. This study was facilitated by the cores of the NIDDK-funded Yale Cooperative Center of Excellence in Hematology (U54DK106857). J.L. is partly supported by NIH grants R01AI181308, R01CA256530, R33CA246711, R01GM138856, and R01DK129523. Y.A. is supported by an NSF GRFP fellowship. L.T. is supported by the Paul Frenette Scholar Award from the Stem Cell Institute of the Albert Einstein College of Medicine. P.K. is partly supported by NIH grant R01AI145164.

AUTHOR CONTRIBUTIONS

J.L. and N.Z. conceived the study. J.L. and D.W. supervised the overall study. N.Z. performed most of the molecular experiments. N.Z. and W.T. performed most of the neutrophil functional studies. L.T. and A.H. designed, performed, and analyzed results from the intravital imaging experiments, assisted by N.Z. and W.T. X.W., D.Z., and J.L. performed computational analysis. Y.A., Y.L., H.Z., Y.W., and V.K. assisted in the experiments. L.Z. assisted on *in vivo* studies and flow cytometry, supervised by P.K. N.Z., W.T., L.T., Y.A., X.W., S.K., A.H., D.W., and J.L. wrote the manuscript.

DECLARATION OF INTERESTS

The authors declare no competing interests.

Received: March 27, 2023

Revised: October 30, 2023

Accepted: December 28, 2023

Published: January 22, 2024

REFERENCES

- Huang, N., Fan, X., Zaleta-Rivera, K., Nguyen, T.C., Zhou, J., Luo, Y., Gao, J., Fang, R.H., Yan, Z., Chen, Z.B., et al. (2020). Natural display of nuclear-encoded RNA on the cell surface and its impact on cell interaction. *Genome Biol.* *21*, 225.
- Flynn, R.A., Pedram, K., Malaker, S.A., Batista, P.J., Smith, B.A.H., Johnson, A.G., George, B.M., Majzoub, K., Villalta, P.W., Carette, J.E., et al. (2021). Small RNAs are modified with N-glycans and displayed on the surface of living cells. *Cell* *184*, 3109–3124.e22.
- Wang, G.G., Calvo, K.R., Pasillas, M.P., Sykes, D.B., Häcker, H., and Kamps, M.P. (2006). Quantitative production of macrophages or neutrophils *ex vivo* using conditional Hoxb8. *Nat. Methods* *3*, 287–293.
- Orosz, A., Walzog, B., and Mócsai, A. (2021). In vivo functions of mouse neutrophils derived from HoxB8-transduced conditionally immortalized myeloid progenitors. *J. Immunol.* *206*, 432–445.
- McDonald, J.U., Cortini, A., Rosas, M., Fossati-Jimack, L., Ling, G.S., Lewis, K.J., Dewitt, S., Liddiard, K., Brown, G.D., Jones, S.A., et al. (2011). In vivo functional analysis and genetic modification of in vitro-derived mouse neutrophils. *FASEB J.* *25*, 1972–1982.
- Chu, J.Y., McCormick, B., Mazelyte, G., Michael, M., and Vermeren, S. (2019). HoxB8 neutrophils replicate Fcγ receptor and integrin-induced neutrophil signaling and functions. *J. Leukoc. Biol.* *105*, 93–100.
- Saul, S., Castelbou, C., Fickentscher, C., and Demaurex, N. (2019). Signaling and functional competency of neutrophils derived from bone-marrow cells expressing the ER-HOXB8 oncoprotein. *J. Leukoc. Biol.* *106*, 1101–1115.
- Filippi, M.D. (2019). Neutrophil transendothelial migration: updates and new perspectives. *Blood* *133*, 2149–2158.
- Vestweber, D., and Blanks, J.E. (1999). Mechanisms that regulate the function of the selectins and their ligands. *Physiol. Rev.* *79*, 181–213.
- Mayadas, T.N., Johnson, R.C., Rayburn, H., Hynes, R.O., and Wagner, D.D. (1993). Leukocyte rolling and extravasation are severely compromised in P selectin-deficient mice. *Cell* *74*, 541–554.
- Labow, M.A., Norton, C.R., Rumberger, J.M., Lombard-Gillooly, K.M., Shuster, D.J., Hubbard, J., Bertko, R., Knaack, P.A., Terry, R.W., and Harbison, M.L. (1994). Characterization of E-selectin-deficient mice: demonstration of overlapping function of the endothelial selectins. *Immunity* *1*, 709–720.
- Sako, D., Chang, X.J., Barone, K.M., Vachino, G., White, H.M., Shaw, G., Veldman, G.M., Bean, K.M., Ahern, T.J., and Furie, B. (1993). Expression cloning of a functional glycoprotein ligand for P-selectin. *Cell* *75*, 1179–1186.
- Xia, L., Sperandio, M., Yago, T., McDaniel, J.M., Cummings, R.D., Pearson-White, S., Ley, K., and McEver, R.P. (2002). P-selectin glycoprotein ligand-1-deficient mice have impaired leukocyte tethering to E-selectin under flow. *J. Clin. Invest.* *109*, 939–950.
- McEver, R.P., and Zhu, C. (2010). Rolling cell adhesion. *Annu. Rev. Cell Dev. Biol.* *26*, 363–396.
- Nourshargh, S., and Alon, R. (2014). Leukocyte migration into inflamed tissues. *Immunity* *41*, 694–707.
- Shih, J.D., and Hunter, C.P. (2011). SID-1 is a dsRNA-selective dsRNA-gated channel. *RNA* *17*, 1057–1065.
- Feinberg, E.H., and Hunter, C.P. (2003). Transport of dsRNA into cells by the transmembrane protein SID-1. *Science* *301*, 1545–1547.
- Duxbury, M.S., Ashley, S.W., and Whang, E.E. (2005). RNA interference: A mammalian SID-1 homologue enhances siRNA uptake and gene silencing efficacy in human cells. *Biochem. Biophys. Res. Commun.* *337*, 459–463.
- Chen, Q., Zhang, F., Dong, L., Wu, H., Xu, J., Li, H., Wang, J., Zhou, Z., Liu, C., Wang, Y., et al. (2021). SIDT1-dependent absorption in the stomach mediates host uptake of dietary and orally administered microRNAs. *Cell Res.* *31*, 247–258.
- Aizawa, S., Fujiwara, Y., Contu, V.R., Hase, K., Takahashi, M., Kikuchi, H., Kabuta, C., Wada, K., and Kabuta, T. (2016). Lysosomal putative RNA transporter SIDT2 mediates direct uptake of RNA by lysosomes. *Autophagy* *12*, 565–578.
- Takahashi, M., Contu, V.R., Kabuta, C., Hase, K., Fujiwara, Y., Wada, K., and Kabuta, T. (2017). SIDT2 mediates gymnosis, the uptake of naked single-stranded oligonucleotides into living cells. *RNA Biol.* *14*, 1534–1543.
- Pouyani, T., and Seed, B. (1995). PSGL-1 recognition of P-selectin is controlled by a tyrosine sulfation consensus at the PSGL-1 amino terminus. *Cell* *83*, 333–343.
- Sako, D., Comess, K.M., Barone, K.M., Camphausen, R.T., Cumming, D.A., and Shaw, G.D. (1995). A sulfated peptide segment at the amino terminus of PSGL-1 is critical for P-selectin binding. *Cell* *83*, 323–331.
- Varki, A. (1997). Selectin ligands: will the real ones please stand up? *J. Clin. Invest.* *99*, 158–162.
- Aruffo, A., Kolanus, W., Walz, G., Fredman, P., and Seed, B. (1991). CD62/P-selectin recognition of myeloid and tumor cell sulfatides. *Cell* *67*, 35–44.
- Yang, J., Hirata, T., Croce, K., Merrill-Skoloff, G., Tchernychev, B., Williams, E., Flaumenhaft, R., Furie, B.C., and Furie, B. (1999). Targeted gene disruption demonstrates that P-selectin glycoprotein ligand 1 (PSGL-1) is required for P-selectin-mediated but not E-selectin-mediated neutrophil rolling and migration. *J. Exp. Med.* *190*, 1769–1782.
- Nguyen, T.A., Smith, B.R.C., Tate, M.D., Belz, G.T., Barrios, M.H., Elgass, K.D., Weisman, A.S., Baker, P.J., Preston, S.P., Whitehead, L., et al. (2017). SIDT2 transports extracellular dsRNA into the cytoplasm for innate immune recognition. *Immunity* *47*, 498–509.e6.
- Nguyen, T.A., Smith, B.R.C., Elgass, K.D., Creed, S.J., Cheung, S., Tate, M.D., Belz, G.T., Wicks, I.P., Masters, S.L., and Pang, K.C. (2019). SIDT1 localizes to endolysosomes and mediates double-stranded RNA transport into the cytoplasm. *J. Immunol.* *202*, 3483–3492.
- Ma, Y., Guo, W., Mou, Q., Shao, X., Lyu, M., Garcia, V., Kong, L., Lewis, W., Ward, C., Yang, Z., et al. (2023). Spatial imaging of glycoRNA in single cells with ARPLA. *Nat. Biotechnol.*
- Schindelin, J., Arganda-Carreras, I., Frise, E., Kaynig, V., Longair, M., Pietzsch, T., Preibisch, S., Rueden, C., Saalfeld, S., Schmid, B., et al. (2012). Fiji: An open-source platform for biological-image analysis. *Nat. Methods* *9*, 676–682.
- Cheng, J., Guo, S., Chen, S., Mastriano, S.J., Liu, C., D'Alessio, A.C., Hysolli, E., Guo, Y., Yao, H., Megyola, C.M., et al. (2013). An extensive network of TET2-targeting MicroRNAs regulates malignant hematopoiesis. *Cell Rep.* *5*, 471–481.
- Roden, C., Gaillard, J., Kanoria, S., Rennie, W., Barish, S., Cheng, J., Pan, W., Liu, J., Cotsapas, C., Ding, Y., et al. (2017). Novel determinants of mammalian primary microRNA processing revealed by systematic evaluation of hairpin-containing transcripts and human genetic variation. *Genome Res.* *27*, 374–384.
- Paik, J.H., Skoura, A., Chae, S.S., Cowan, A.E., Han, D.K., Proia, R.L., and Hla, T. (2004). Sphingosine 1-phosphate receptor regulation of N-cadherin mediates vascular stabilization. *Genes Dev.* *18*, 2392–2403.
- Cao, J., Wu, L., Zhang, S.-M., Lu, M., Cheung, W.K.C., Cai, W., Gale, M., Xu, Q., and Yan, Q. (2016). An easy and efficient inducible CRISPR/Cas9 platform with improved specificity for multiple gene targeting. *Nucleic Acids Res.* *44*, e149.
- Doench, J.G., Fusi, N., Sullender, M., Hegde, M., Vaimberg, E.W., Donovan, K.F., Smith, I., Tothova, Z., Wilen, C., Orchard, R., et al. (2016). Optimized sgRNA design to maximize activity and minimize off-target effects of CRISPR-Cas9. *Nat. Biotechnol.* *34*, 184–191.

36. Adams, B.D., Guo, S., Bai, H., Guo, Y., Megyola, C.M., Cheng, J., Heydari, K., Xiao, C., Reddy, E.P., and Lu, J. (2012). An in vivo functional screen uncovers miR-150-mediated regulation of hematopoietic injury response. *Cell Rep.* 2, 1048–1060.
37. Zhang, Y., Tang, W., Jones, M.C., Xu, W., Halene, S., and Wu, D. (2010). Different roles of G protein subunits beta1 and beta2 in neutrophil function revealed by gene expression silencing in primary mouse neutrophils. *J. Biol. Chem.* 285, 24805–24814.
38. Xu, W., Wang, P., Petri, B., Zhang, Y., Tang, W., Sun, L., Kress, H., Mann, T., Shi, Y., Kubes, P., et al. (2010). Integrin-induced PIP5K1C kinase polarization regulates neutrophil polarization, directionality, and in vivo infiltration. *Immunity* 33, 340–350.
39. Wang, N., Cheng, J., Fan, R., and Lu, J. (2017). Capture, amplification, and global profiling of microRNAs from low quantities of whole cell lysate. *Analyst* 142, 3203–3211.
40. Wang, N., Zheng, J., Chen, Z., Liu, Y., Dura, B., Kwak, M., Xavier-Ferrucio, J., Lu, Y.C., Zhang, M., Roden, C., et al. (2019). Single-cell microRNA-mRNA co-sequencing reveals non-genetic heterogeneity and mechanisms of microRNA regulation. *Nat. Commun.* 10, 95.
41. Guo, Y., Liu, J., Elfenbein, S.J., Ma, Y., Zhong, M., Qiu, C., Ding, Y., and Lu, J. (2015). Characterization of the mammalian miRNA turnover landscape. *Nucleic Acids Res.* 43, 2326–2341.

STAR★METHODS

KEY RESOURCES TABLE

REAGENT or RESOURCE	SOURCE	IDENTIFIER
Antibodies		
Anti-P-selectin	Biologend	Cat# 148302; RRID: AB_2564111
Anti-E-selectin	eBioscience	Cat# 14-0627-82; RRID: AB_2864911
Anti-Sid1 antibody	Thermo Fisher	Cat# 55352-1-AP; RRID: AB_11182721
Anti-Sid2 antibody	Thermo Fisher	Cat# PA5-34493; RRID: AB_2551845
Anti-beta Actin antibody	Abcam	Cat# ab8227; RRID: AB_2305186
PE anti-mouse CD11b antibody	BD Biosciences	Cat# 561689; RRID: AB_10893803
Pacific Blue anti-mouse Ly6G antibody	Biologend	Cat# 127612; RRID: AB_2251161
FITC Goat anti-Human IgG-Fc antibody	Sigma	Cat# F9512; RRID: AB_259808
PE-Cy7 anti-mouse CD11a	BD Biosciences	Cat# 558191; RRID: AB_397055
Pacific Blue anti-mouse/human CD11b	Biologend	Cat# 101223; RRID: AB_755985
Cy5-conjugated AffiniPure goat anti-human Fc γ fragment-specific IgG F(ab') ₂ fragments	Jackson Immunobiology	Cat# 109-176-098
BV711 anti-mouse PSGL-1	BD Biosciences	Cat# 740746; RRID: AB_2740414
PE anti-mouse L-selectin	BD Biosciences	Cat# 561918; RRID: AB_10894006
HRP-linked antibody anti-biotin	Cell Signaling Technology	Cat# 7075; RRID: AB_10696897
HRP-linked goat anti-human IgG-Fc	Thermo Fisher	Cat# 31413; RRID: AB_429693
Biotin-labeled anti-BrdU antibody	Biologend	Cat# 317904; RRID: AB_604041
Bacterial and virus strains		
Competent <i>E. coli</i> (DH5a)	Thermo Fisher	Cat# 18265017
Chemicals, peptides, and recombinant proteins		
BsmBI	NEB	Cat# R0580
Esp3I	NEB	Cat# R0734L
T4 DNA ligase	NEB	Cat# M0202L
Ficoll Paque Plus	Cytiva	Cat# 17144002
Percoll	Cytiva	Cat# 17089101
DMSO	americanBio	Cat# AB03091
IL3	Peprotech	Cat# 213-13
SCF	Peprotech	Cat# 250-03
IL6	Biologend	Cat# 575702
β -estradiol	Sigma	Cat# E2758
PBS	Corning	Cat# 21-031-CV
May-Grunwald Solution	Sigma Aldrich	Cat# 63590
Giemsa Stain Modified Solution	Sigma Aldrich	Cat# 48900
HEPES	Gibco	Cat# 15630080
N-azidoacetylmannosamine-tetraacylated, (Ac4ManNAz)	Click Chemistry Tools	Cat# 1084
N-Acetyl-D-galactosamine (GalNAc)	Sigma	Cat# A2795
D-(+)-Galactose (Gal)	Sigma	Cat# G0750
TRIzol	Thermo Fisher	Cat# 15596
Proteinase K (Pro K)	Thermo Fisher	Cat# 25530049
RNase A	Roche	Cat# 10109169001
RNase Inhibitor	NEB	Cat# M0314
DEPC	Sigma	Cat# D5758

(Continued on next page)

Continued

REAGENT or RESOURCE	SOURCE	IDENTIFIER
DNase I	Roche	Cat# 04716728001
PNGase F	NEB	Cat# P0704
GlycoBuffer 2 (NEB, #B3704)	NEB	Cat# B3704
Dibenzocyclooctyne-PEG4-biotin (DBCO-PEG4-biotin)	Sigma	Cat# 760749
SYBR Gold	Thermo Fisher	Cat# S11494
0.45 μ m nitrocellulose membrane	Bio-Rad	Cat# D101563
Odyssey Blocking Buffer, PBS	Li-Cor Biosciences	Cat# 927-70001
Tween-20	Sigma	Cat# P1379
TBS buffer	Bio-Rad	Cat#1706435
Immobilon Crescendo Western HRP substrate	Millipore	Cat# 42029053
P-selectin-Fc	Biolegend	Cat# 755404
E-selectin-Fc	Biolegend	Cat# 755502
BrU	Sigma	Cat# 850187
granulocyte-macrophage colony-stimulating factor (GM-CSF)	PeproTech	Cat# 315-03
Hoechst 33342	Thermo Fisher	Cat# H3570
streptavidin-FITC (SAv-FITC)	Biolegend	Cat# 405201
CFSE	Thermo Fisher	Cat# V12883
Far-Red DDAO SE	Thermo Fisher	Cat# C34553
HBSS, no calcium, no magnesium	Gibco	Cat# 14175103
HBSS, calcium, magnesium	Gibco	Cat# 14025076
Thioglycolate	Sigma	Cat# 70157
LPS E. Coli O111:B4	Sigma	Cat# LPS25
fMLP	Sigma	Cat# F3506
Cytox Red	Thermo Fisher	S34859
6.5 mm Transwell® with 5.0 μ m Pore Polycarbonate Membrane Insert	Corning	Corning, #3421
TNF- α (PeproTech, #315-01A)	PeproTech	Cat# 315-01A
ICAM-1-Fc	R&D Systems	Cat# 796-IC
BSA	Sigma	Cat# A9647
Poly-D-lysine (0.1 mg/mL, Gibco, #881772H)	Gibco	Cat# 881772H
Parallel plate flow chamber	GlycoTech	Cat# 31001
MyOne C1 Streptavidin beads	Thermo Fisher	Cat# 65001
glycogen	Thermo Fisher	Cat# R0551
Wheat germ agglutinin (WGA) agarose beads	Vector Laboratories	Cat# AL-1023
Elution Buffer	Pierce	Cat# 1859690
enzyme-free cell dissociation buffer	Gibco	Cat# 13151014
Fibrinogen	Sigma	Cat# F3879
Paraformaldehyde (PFA)	Electron Microscopy Science	Cat# 15710
Chloroform	Sigma	Cat# C2432
DMEM medium	Thermo Fisher	Cat# 11995-065
RPMI medium	Thermo Fisher	Cat#11875-093
Fetal Bovine Serum (FBS)	Thermo Fisher	Cat# 10438-026
Penicillin-streptomycin and glutamine	Thermo Fisher	Cat# 10378-016
Puromycin	Gibco	Cat# A1113803
0.45 μ m nitrocellulose membrane	Bio-Rad	Cat #1620094

(Continued on next page)

Continued		
REAGENT or RESOURCE	SOURCE	IDENTIFIER
SSC buffer	Sigma	Cat# S6639
Odyssey Blocking Buffer, PBS	Li-Cor Biosciences	Cat# 927-70001
TNF- α	R&D Systems	Cat# 410-MT-025
α -chloralose	Sigma	Cat# C0128-25G
Urethane	Sigma	Cat# 76607
PE-10 catheter	BD Intramedic™	Cat# 427400
Critical commercial assays		
QIAprep Spin Miniprep Kit	Qiagen	Cat# 27106
TruSeq Small RNA Kit	Illumina	Cat# 20005613
Deposited data		
RNA-seq and small RNA seq data	Gene Expression Omnibus	GEO: GSE224128
Experimental models: Cell lines		
293T	ATCC	Cat# CRL-3216
Endothelial cells	Timothy Hla Lab	N/A
HOXB8	This study	N/A
Experimental models: Organisms/strains		
C57BL/6 mouse	The Jackson Laboratory	Strain #:000664
Cas9-GFP mouse	The Jackson Laboratory	Strain #:026179
JAXBoy mouse	The Jackson Laboratory	Strain #:033076
Oligonucleotides		
See Table S3		
Recombinant DNA		
pXPR_050 vector	Addgene	Cat# 96925
LentiCas9-blast	Addgene	Cat# 52962
Software and algorithms		
DESeq2	Bioconductor	https://bioconductor.org/packages/release/bioc/html/DESeq2.html
ImageJ	NIH	https://imagej.net/ij/index.html
Fiji	Schindelin et al. ³⁰	https://fiji.sc/
Adobe Illustrator	Adobe	https://www.adobe.com/products/illustrator.html
FlowJo	FlowJo, LLC	https://www.flowjo.com/
Other		
Custom Codes	Github	https://github.com/YaleLuLab/Neutrophil_RNA.git

RESOURCE AVAILABILITY

Lead contact

Further information and requests for resources and reagents should be directed to and will be fulfilled by the [lead contact](#), Jun Lu (jun.lu@yale.edu).

Materials availability

All plasmids generated in this study are available upon request. All cell lines generated in this study are available upon request.

Data and code availability

Data

Next generation sequencing data have been deposited at GEO and are publicly available as of the date of publication. Accession numbers are listed in the [key resources table](#).

Code

All original code has been deposited at github and is publicly available as of the date of publication. Website to the code is listed in the [key resources table](#).

Any additional information required to reanalyze the data reported in this paper is available from the [lead contact](#) upon request.

EXPERIMENTAL MODEL AND STUDY PARTICIPANT DETAILS

Mice

All animal experiments were performed in accordance with the guidelines of Yale University's Institutional Animal Care and Use Committee. C57BL/6J mice, Cas9-GFP, and JAXBoy mice were purchased from the Jackson Laboratory. Unless otherwise specified, wild-type female mice of ~6–8 weeks of age were used as recipients for neutrophil transfer. Both wild-type and Cas9-GFP mice were used as donors for deriving HOXB8 cells. Wild-type mice were used as donors of primary neutrophils.

Cell culture

293T cells were originated from ATCC, and cultured in the DMEM medium (Thermo Fisher) with 10% FBS (Thermo Fisher) and 1% penicillin-streptomycin and glutamine (Thermo Fisher,). Lentiviruses were prepared following our previous methods using 293T cells.^{31,32}

Two HOXB8 lines were derived from bone marrow cells of a wildtype CD45.1 C57BL/6 mouse and a Cas9-GFP mouse, respectively, according to a published procedure.³ Briefly, bone marrow cells were enriched for progenitors using Ficoll Paque Plus (Cytiva) and cultured for 2 days in RPMI medium (Thermo Fisher) with 10% FBS (Thermo Fisher), 1% penicillin-streptomycin and glutamine (Thermo Fisher), and 10 ng/ml of murine IL3 (Peprotech), murine SCF (Peprotech), and murine IL6 (Biolegend). Cells were then infected with Hoxb8-ER-neo and further cultured in HOXB8 cell growth medium: RPMI medium (Thermo Fisher) with 10% FBS (Thermo Fisher) and 1% penicillin-streptomycin and glutamine (Thermo Fisher), supplemented with 1 μ M β -estradiol (Sigma) and 100 ng/ml recombinant murine SCF (Peprotech). Immortalized lines could be derived after 2 weeks of culture. To differentiate into neutrophils, HOXB8 cells were washed two to three times with phosphate-buffered saline (PBS, Corning) and cultured in the differentiation medium (same as the growth medium but without β -estradiol). Cells from 2 to 4 days of differentiation culture were used for experiments.

Mouse endothelial cells used were immortalized murine embryonic (E12.5) endothelial cells,³³ kindly provided by Dr. Timothy Hla. These cells were cultured in DMEM medium (Thermo Fisher) with 10% FBS (Thermo Fisher), 1% penicillin-streptomycin and glutamine (Thermo Fisher) and 10 mM HEPES (Gibco).

METHOD DETAILS

Plasmids

All primers, synthetic DNA sequences, and sgRNA sequences used for cloning are listed in [Table S3](#). Oligonucleotides were ordered from IDT. Synthetic DNA fragments were ordered from Twist Bioscience.

For generating HOXB8 cells, a retroviral vector encoding Hoxb8-ER and neomycin resistance were kindly provided by Dr. David Sykes.

To generate sgRNAs against *Sid1*, *Sid2*, and *Selp*, we generated multi-sgRNA vectors following a published strategy.³⁴ We obtained the sgRNA sequences for *Sid1*, *Sid2*, *Selp*, or nontargeting controls from the published Brie library.³⁵ We obtained PCR products with sgRNA sequences flanking a synthetic v2-tracrRNA-U6 fragment, with PCR primers also containing BsmBI/Esp3I sites. These PCR fragments were cloned into the pXPR_050 vector (Addgene #96925) with v2 tracrRNA, by first digestion with BsmBI and gel-purification of the vector, followed by a Golden Gate assembly reaction. The Golden Gate assembly was performed in a 10 μ l total reaction volume with 30 ng of the purified vector, PCR fragments each being 3 times the molar quantity of the vector, 1 μ l 10x T4 ligase buffer, 6 U Esp3I (NEB), and 400 U T4 DNA ligase (NEB). Reaction was incubated at 37°C for 5 minutes and 16°C for 5 minutes for each cycle with a total of 30 cycles.

The LentiCas9-blast vector was obtained from Addgene (#52962).

Generating KO or KD cells

CRISPR against *Sid1* and *Sid2* was carried out by lentiviral infection of Cas9-GFP HOXB8 cells with control or sgRNA vectors against *Sid1* and/or *Sid2*. Infection was performed by spin-infection following our previous methods.³⁶ Cells were then selected with puromycin. The pools of selected cells were then used for experiments. To generate P-selectin KO ECs, ECs were infected with lentivirus for LentiCas9-blast, and then with lentivirus for sgRNAs against P-selectin. Infected cells were cultured for >7 days, and briefly treated with TNF α before FACS-sorting based on staining by the anti-P-selectin antibody to obtain P-selectin negative cells. These *Selp* KO cells were confirmed by western blot to have lost P-selectin expression.

Neutrophil isolation from bone marrow

Murine neutrophils were purified from bone marrows as previously described.³⁷ Briefly, bone marrow cells collected from mice were treated with the ACK buffer (155 mM NH₄Cl, 10 mM KHCO₃ and 0.1 mM EDTA) for red blood cell lysis, followed by a discontinuous Percoll (Cytiva) density gradient centrifugation. Neutrophils were collected from the band located between 81% and 62% of Percoll.

May-Grunwald-Giemsa staining

May-Grunwald-Giemsa staining was performed using the May-Grunwald Solution (Sigma-Aldrich) and Giemsa Stain Modified Solution (Sigma-Aldrich) following manufacturer's protocol. Briefly, cells were cytospun onto glass slides, allowed to air-dry for 2 minutes, and immediately stained in May-Grunwald solution for 5 minutes. Slides were washed in PBS (Corning) for 1.5 minutes, followed by staining in 1:20 diluted Giemsa Solution in distilled water for 20 minutes. Slides were then washed in distilled water and imaged.

Ac₄ManNAz treatment

N-azidoacetylmannosamine-tetraacylated (Ac₄ManNAz, Click Chemistry Tools) was dissolved at a 500 mM working stock in sterile dimethyl sulfoxide (DMSO). N-Acetyl-D-galactosamine (GalNAc, Sigma) and D-(-)-Galactose (Gal, Sigma) were prepared for 500 mM and 50 mM working stocks, respectively, in sterile water. To label the cells, Ac₄ManNAz was used at a final concentration of 100 μM in the culture medium supplemented with Gal and GalNAc at 10 μM and 100 μM, respectively. Treatment was performed for 36 hours unless specified otherwise.

RNA extraction and purification

The cells were washed twice by PBS. TRIzol (Thermo Fisher Scientific) was used to lyse and denature the cells. After homogenization in TRIzol by pipetting up and down, samples were incubated at 37°C for 15 min to further disrupt non-covalent interactions. Chloroform extraction and isopropanol precipitation were performed according to manufacturer's protocol. The RNA pellet was dissolved in RNase-free water and subjected to protein digestion by adding 1 μg of Proteinase K (Pro K, Thermo Fisher Scientific) to 1 μg of purified RNA and incubating for 30 minutes at 37°C. After Pro K digestion, RNA was purified again with TRIzol as described above. All RNA samples generated in this study were purified by these two steps first, unless specified otherwise, before subsequent enzymatic treatment or biotin labeling.

Enzymatic treatment of RNA samples and cells

Various endo- and exonucleases and glycosidases were used to digest RNA, DNA, or glycans. To digest purified RNA, unless specified otherwise, 1 μL of RNase A (20 mg/mL, Roche) was added to 20 μg RNA in a 20 μL volume with 20 mM Tris-HCl (pH 7.5), 100 mM KCl and 0.1 mM MgCl₂ and incubated at 37°C for 60 minutes. To digest the extracellular RNA on the cell surface, the cells were washed twice with PBS and re-suspended in PBS, extracellular RNase A was added to a final concentration of 0.1 mg/mL in PBS and incubated at 37°C for 10 minutes. During the digestion, the tube was inverted gently once every 2 minutes to prevent the cells from clumping at the bottom. To block the RNase A activity when digesting purified RNAs, 1 μg of RNase A was pre-incubated with 10 μL of RNase Inhibitor (40U/μL, NEB) for 30 min at 25°C before adding to the RNA solution. For *in vivo* experiments involving inactivated RNase A, we initially tried to use protein-based RNase Inhibitor, but the amount of RNase Inhibitor required could cause neutrophil behavior changes. Instead, RNase A was pre-incubated with 0.1% DEPC for overnight on rotation and autoclaved at 121°C for 30 minutes, before cooling down to room temperature gradually to allow protein renaturation. Of note, RNase A (without DEPC treatment) that underwent similar procedures recovered most of its activity following renaturation. To digest DNA, 1 μL DNase I (10U/μL, Roche) was added to a 20 μL reaction volume with 20 mM Tris-HCl (pH 7.4), 50 mM NaCl, 2 mM CaCl₂, 2 mM MgCl₂ at 37°C for 60 minutes. To digest protein, 2 μL of Pro K (20 mg/mL) was added to a 20 μL reaction volume with 20 mM Tris-HCl (pH 7.5), 2 mM CaCl₂ and 0.2% SDS at 37°C for 60 min. To digest the protein on the cell surface, the cells were washed twice with PBS and resuspended in PBS, Pro K was pre-incubated at 37°C for 5 minutes to eliminate any possible contamination of RNase and then added to a final concentration of 0.01 mg/mL into the cell suspension and incubated at 37°C for 5 min. Of note, too long or too high a concentration of Pro K digestion will result in loss of cell surface RNA signals, presumably due to the release of RNAs by the protecting protein(s). To digest the glycans from glycoRNA, 2 μL PNGase F (500U/μL, NEB) was added to total RNA (20 μg) or purified glycoRNA in a 20 μL reaction volume with 1 × GlycoBuffer 2 (NEB) and incubated at 37°C for 60 min. After enzymatic digestions of a RNA sample, the reaction was purified with TRIzol extraction and precipitation before further analysis.

Copper-free click chemistry reaction

Dibenzocyclooctyne-PEG₄-biotin (DBCO-PEG₄-biotin, Sigma), was used for labeling azide containing molecules or compounds under copper-free conditions. To perform the biotin labeling, RNA in RNase-free water was mixed with 1 × volumes of "dye-free" Gel Loading Buffer II (df-GLBII, 95% Formamide, 18mM EDTA, and 0.025% SDS) and 500 μM DBCO-PEG₄-biotin. Samples were conjugated at 50°C for 5 min. Reaction was stopped by adding 2.5 × volumes of ethanol for precipitation. The biotin-labeled RNA was treated enzymatically as described above or analyzed by gel electrophoresis as described below. To label the azide containing molecules or compounds on the cell surface, DBCO-PEG₄-biotin was added into PBS suspended cells at a final concentration of 500 μM and incubated at 37°C for 20 min, the reaction was stopped by washing away the free DBCO-PEG₄-biotin with PBS.

RNA gel electrophoresis, blotting, and imaging

Blotting analysis of Ac₄ManNAz-labeled RNA was performed similar to a northern blot with the following modifications. Purified, enriched, or enzymatically treated RNAs were conjugated to DBCO-PEG₄-biotin as described above. The labeled RNA was resuspended in 10 μL df-GLBII with SYBR Gold (Thermo Fisher Scientific). To denature RNA, RNA samples were incubated at 50°C for 5 min and chilled on ice for 3 min. Samples were then loaded to a 1% agarose formaldehyde-denaturing gel and electrophoresed

in 1 × MOPS buffer. The RNA in the gel was imaged using gel imager. The RNA was then transferred to 0.45 μm nitrocellulose membrane (Bio-Rad) following the northern blot procedure for 16 hours at 4°C using 1 × SSC buffer (Sigma). After transfer, RNA was cross-linked to the nitrocellulose membrane using UV-C light (0.18 J/cm²). The membrane was then blocked with Odyssey Blocking Buffer, PBS (Li-Cor Biosciences) for 60 min at 4°C. After blocking, HRP-linked antibody anti-biotin (Cell Signaling Technology) was diluted to 1:2,500 in Odyssey Blocking Buffer and incubated with the membrane for 2 hours at 4°C. Excess antibody was washed from the membranes by three washes of 0.1% Tween-20 (Sigma) in 1 × TBS buffer (Bio-Rad) for 10 minutes each at 4°C. The membrane was briefly rinsed in 1 × TBS to remove the Tween-20 and imaged by using Immobilon Crescendo Western HRP substrate (Millipore). For the blot analysis of P-/E-selectin-Fc, total RNA without Ac₄ManNAz labeling was transferred to a nitrocellulose membrane, and the membrane was incubated with recombinant mouse P-/E-selectin-Fc (Biolegend) at 1:500 dilution and HRP-linked goat anti-human IgG-Fc (Thermo Fisher) at 1:2000 dilution.

Imaging of cell surface RNAs

To label the RNA, BM neutrophils were cultured in RPMI medium (Thermo Fisher) with 10% FBS (Thermo Fisher) and 1% penicillin-streptomycin and glutamine (Thermo Fisher), supplemented with 20 mM BrU (Sigma) and 25 ng/mL granulocyte-macrophage colony-stimulating factor (GM-CSF, PeproTech) for 24 hours. After labeling, neutrophils were further cultured in the culture medium supplemented with 5 μg/mL Hoechst 33342 (Thermo Fisher Scientific) for 30 minutes to stain the cellular DNA. Cells were treated extracellularly with proteinase K (exPro K) or with mock treatment as described above. Cells then underwent exRNaseA or mock treatment as described above. To stain the cell surface RNA, biotin-labeled anti-BrdU antibody (Biolegend, also recognizes BrU) was pre-incubated with streptavidin-FITC (SAV-FITC, Biolegend) at a 1:1 ratio for 30 min at 25°C. Neutrophils were incubated with a 1:100 dilution of SAV-FITC pre-incubated biotin-labeled anti-BrdU Antibody in PBS supplemented with 2% FBS at 37°C for 10 minutes. Excess antibody was washed away twice by culture medium. Images were captured on a STELLARIS 5 Confocal Microscope (Leica). To limit the movement of live neutrophils during confocal imaging, we added the cells into 35 mm cell culture plates (MatTek) which were printed with microwells of 300 to 500 microns in size by a prototype TROVO machine from Enrich Biosystems.

Analysis of neutrophil recruitment *in vivo*

Neutrophil recruitment *in vivo* was assessed using an acute peritonitis model and an acute lung inflammation model. The purified bone marrow neutrophils were treated as specified in the figure legends and labeled with either 1 μM CFSE (Thermo Fisher) or 1 μM Far-Red DDAO SE (Thermo Fisher) in HBSS without Ca²⁺/Mg²⁺. After 15 minutes incubation at 37°C for labeling, cells were washed twice with HBSS without Ca²⁺/Mg²⁺. These two dyes-labeled neutrophils were mixed in a 1:1 ratio and about 10 million total cells were injected retro-orbitally into WT recipient mice, which had previously received an intraperitoneal injection of 1.5 ml of 3% thioglycolate (Sigma) 1.5 hours prior or an intranasal injection of 50 μg LPS (E. Coli O111:B4, Sigma, LPS25) 16 hours prior. For the peritonitis model, the mice were then euthanized 2.5 or 6 hours later, and cells in the peritoneum, blood, spleen, bone marrow were collected and analyzed through cell counting and flow cytometry. For the lung model, the mice were euthanized 2.5 hours after the retro-orbital transfer of neutrophils and cells in the blood and bronchoalveolar lavage (BAL) were collected and analyzed through cell counting and flow cytometry. To collect cells in the BAL, 1 ml of PBS was instilled into the lungs and retrieved via a tracheal catheter to obtain BAL. Neutrophils were identified through double-positive staining with PE anti-mouse CD11b antibody (BD Biosciences) and Pacific Blue anti-mouse Ly6G antibody (Biolegend), and in some experiments, with Ly6G positivity alone. To eliminate dye effects, dye swapping experiments were also performed.

For experiments to evaluate the *in vivo* survival of exRNaseA treated neutrophils, similar experiments as those for the acute peritonitis model were performed, except that cells were injected directly into the thioglycolate treated peritoneum.

To perform *Sid1*-KO neutrophil recruitment assay *in vivo*, control sgRNA HOXB8 cells (CD45.2, GFP⁺), *Sid1*-KD#1, or *Sid1*-KD#2 HOXB8 cells (CD45.2, GFP⁺) were transferred to lethally irradiated JAXBoy (CD45.1) mice via retro-orbital injection with ~30 million cells per mouse. Five days after the transfer, reconstituted control or *Sid1*-KD neutrophils were directly collected from bone marrow. Control neutrophils were labeled with 1 μM Far-Red DDAO SE (Thermo Fisher) in HBSS without Ca²⁺/Mg²⁺. The dye-labeled control neutrophils were mixed with *Sid1*-KD neutrophils at a 1:1 ratio and injected retro-orbitally into wild-type recipient mice, which had previously received an intraperitoneal injection of 1.5 ml of 3% thioglycolate (Sigma) 1.5 hours prior. The mice were then euthanized 2.5 hours later, and cells in the peritoneum and blood were collected and analyzed through cell counting and flow cytometry. Neutrophils were identified through double-positive staining with a PE anti-mouse CD11b antibody (BD Biosciences) and a Pacific Blue anti-mouse Ly6G antibody (Biolegend).

Analysis of neutrophil plasma membrane integrity

To analyze the neutrophil plasma membrane integrity after exRNaseA treatment, Cytox Red staining was performed. Mock-treated or exRNaseA-treated BM neutrophils were stimulated by 2 μM fMLP in HBSS with Ca²⁺ and Mg²⁺ or by mock for 10 minutes at 37°C. fMLP was washed twice by HBSS with Ca²⁺ and Mg²⁺. Neutrophils were then stained by Cytox Red for 30 minutes in 0.5% BSA in HBSS. To analyze neutrophil plasma membrane integrity in the acute peritonitis model *in vivo*, exRNaseA-treated BM neutrophils were stained by CFSE and injected to TG-treated mice as above described. Peripheral blood and peritoneal neutrophils were harvested after 2.5 hours injection and stained by Cytox Red. Neutrophils were identified by staining with PE anti-CD11b (BD Biosciences) and Pacific Blue anti-Ly6G (Biolegend).

Neutrophil transwell migration *in vitro*

To perform the neutrophil migration assay *in vitro*, transwell chambers with 6.5 mm polycarbonate inserts and 5.0 μm pore size (Corning) were used. To seed the WT or P-selectin KO endothelial cells on the polycarbonate membrane of the top insert, the endothelial cells were cultured in the top insert. When endothelial cells formed a dense layer and completely covered the polycarbonate membrane of the top insert, a final concentration of 50 ng/mL TNF- α (PeproTech) was added to the medium and endothelial cells were cultured for an additional 4 hours. In some conditions the activated endothelial cells were pre-blocked with purified glycoRNA. After activation of TNF- α , the culture medium in the top insert was removed and 0.5×10^6 of purified neutrophils from BM or HOXB8-differentiated neutrophils, suspended in 0.5 mL HBSS with Ca^{2+} and Mg^{2+} (Gibco), were added to the top insert. 0.5 mL of HBSS with Ca^{2+} and Mg^{2+} supplemented with 2 μM fMLP (Sigma) was added to the bottom chamber. Neutrophils migrate assay was performed at 37°C, 5% CO_2 for 2 hours. After the migration of neutrophils to the lower chamber of the wells, cells were collected and counted on a flow cytometer using spike-in counting beads or under microscopy. In certain experiments, no endothelial cells were seeded on the polycarbonate membrane of the top insert, and neutrophils suspended in HBSS with Ca^{2+} and Mg^{2+} were directly added to the top insert. The migrate assay was performed the same as described above.

To test the glycoRNA levels after transwell migration, Ac_4ManNAz -labeled BM neutrophils were subjected to transwell migration at 37°C, 5% CO_2 for 2 hours without ECs and the migrated neutrophils were collected. RNAs from the migrated and control neutrophils (without fMLP and without migration) were extracted, labeled and blotted for glycoRNAs as described in the glycoRNA detection section.

Analysis of neutrophil cell surface integrins, PSGL-1 and L-selectin

The surface expression of integrins in neutrophils was analyzed using flow cytometry. The cells were stimulated with 10 μM fMLP (Sigma) for 0, 2, or 5 minutes at 37°C, followed by the addition 4% paraformaldehyde to stop the reaction. The cells were stained with PE-Cy7 anti-mouse CD11a (BD Biosciences) and Pacific Blue anti-mouse/human CD11b (Biolegend) antibodies and analyzed using flow cytometry.

To evaluate the activation of integrins in neutrophils, the ICAM-binding assay was carried out as previously described.³⁸ The ICAM-1-Fc-F(ab')₂ complexes were generated by incubating Cy5-conjugated AffiniPure goat anti-human Fc γ fragment-specific IgG F(ab')₂ fragments (Jackson Immunobiology) and ICAM-1-Fc (100 $\mu\text{g}/\text{ml}$) for 30 min at 4°C in PBS. Neutrophils, suspended at 0.5×10^6 cells/ml in PBS containing 0.5% BSA, 0.5mM Mg^{2+} and 0.9mM Ca^{2+} , were then mixed with the ICAM-1-Fc-F(ab')₂ complexes in the presence or absence of fMLP for durations specified in the figures or figure legends. The reactions were terminated by adding 4% paraformaldehyde, followed by the addition of 3 ml ice-cold FACS buffer after 5 minutes. The cells were pelleted, resuspended in 300 μl of FACS buffer, and analyzed on a flow cytometer.

To analyze surface expression level of PSGL-1 and L-selectin in neutrophils after exRNaseA treatment, mock-treated and exRNaseA-treated BM neutrophils were stained with BV711 anti-mouse PSGL-1 (BD) and PE anti-mouse L-selectin (BD) and analyzed using flow cytometry.

Neutrophil spreading assay

Fibrinogen (Sigma) was reconstituted in PBS at a concentration of 100 $\mu\text{g}/\text{ml}$. Cell culture dishes were coated with an adequate amount of the fibrinogen solution to cover the surface and incubated at 37°C for 1 hour. Subsequently, the dishes were rinsed twice with water. Primary neutrophils were suspended in the assay buffer (0.5% BSA in HBSS with $\text{Ca}^{2+}/\text{Mg}^{2+}$) at 1 million/ml. Cells were then seeded onto fibrinogen-coated dishes to spread for 15 minutes at 37°C, after which they were fixed with 4% paraformaldehyde (PFA) for 15 minutes. The dishes were washed 3 times with PBS before imaging under an Olympus IX-81 microscope. The percentage of spreading cells and the area of neutrophils were quantified by using Image J.

Analysis of neutrophil adhesion on ECs

To perform the adhesion assay, ECs were seeded on 3 cm tissue culture dishes (Falcon) pre-treated with poly-D-lysine (0.1 mg/mL, Gibco). BM neutrophils were labeled by 1 μM CFSE (Thermo Fisher). When ECs formed a dense layer and completely covered the dish, a final concentration of 50 ng/mL TNF- α (PeproTech) was added to the medium and the ECs were cultured for an additional 4 hours. After the activation of TNF- α , ECs were washed once by HBSS with Ca^{2+} and Mg^{2+} (Gibco). In some conditions the activated ECs were pre-blocked with purified glycoRNA, glycan fraction or RNA fraction of the purified GlycoRNA. ECs were then incubated with 2 mL HBSS with Ca^{2+} and Mg^{2+} supplemented with 1×10^6 exRNaseA treated or mocked (control) dye-labeled neutrophils at 37°C, 5% CO_2 for 10 minutes. Unattached or loosely attached neutrophils were washed away three times by 2 mL each of HBSS with Ca^{2+} and Mg^{2+} . Attached neutrophils were then counted under microscope, with adhesion quantified as the number of neutrophils averaged across at least 10 random imaging fields and normalized to the control. To perform the adhesion assay under flowing condition, parallel plate flow chamber (GlycoTech) was used. 1×10^6 of CFSE labeled BM neutrophils in 2 mL HBSS with Ca^{2+} and Mg^{2+} were flowed through TNF- α activated endothelial cells at a shear stress of 2 dynes/cm², controlled by an automated syringe. Unattached or loosely attached neutrophils were washed away by flowing 0.5 mL HBSS with Ca^{2+} and Mg^{2+} . Attached cells were then counted as described above.

Intravital confocal microscopy

C57BL/6 male mice (12–16 weeks old) were injected intraperitoneally with 0.5 μg of TNF α (R&D Systems) and anesthetized one hour later by intraperitoneal injection of a mixture of 150 mg/kg α -chloralose (Sigma-Aldrich) and 1.2 g/kg urethane (Sigma-Aldrich) in PBS. Tracheal intubation was performed to ensure respiration after anesthesia. A PE-10 catheter (BD) was inserted into the left common carotid artery for injection of a 1:1 mix of mock (control, labeled with Far-red dyes) and exRNaseA-treated neutrophils (labeled with CFSE). The cremaster muscle was gently exteriorized, mounted onto a microscopic stage, and continuously superfused with bicarbonate-buffered saline (Ringer's solution, pH 7.4, 37°C). Approximately 1×10^7 to 2×10^7 total cells were progressively injected into the carotid artery immediately before and during each image acquisition interval. Images of the cremaster microcirculation were captured between 2.5 and 3.5 hours after TNF α administration, under a 10x water-immersion objective, using an Axio Examiner.Z1 microscope (Zeiss) equipped with ORCA-Fusion BT Digital CMOS camera (Hamamatsu) and a CSU-X1 confocal scan head (Yokogawa) with five lasers (405 nm, 488 nm, 561 nm, 642 nm, and 690 nm). Images were captured every 100 milliseconds. Two to four fields containing multiple vessels were recorded per mouse. Images were processed and analyzed using SlideBook6 software (Intelligent Imaging Innovations) and Fiji.³⁰

Neutrophils that remained stationary for at least 30 seconds of elapsed time were considered as stably adherent cells. Neutrophils that rolled or crawled along the vessel wall and did not stay stationary for more than 30 seconds were defined as rolling cell. Free-flowing cells were counted as those passing through the vessels but did not interact with the endothelium or other neutrophils. Neutrophils that transitioned from free-flowing to rolling, kept rolling throughout the imaging interval, or transitioned from rolling to stable adhesion, were counted. Any stable adhesion that occurred before imaging acquisition were not tallied in the counts. For the same dye-labeled color in each vessel, the neutrophil counts were normalized to reflect the fraction of neutrophil in each behavior category, with the total set to 1. Fields containing less than three cells of each color were not considered for further analysis; and adjacent vessels with low counts were pooled to enable proper paired analysis. Statistical comparison used paired t-test.

Label-based and label-free purification of GlycoRNAs

Two different strategies were applied to enrich the biotin-labeled or label-free glycoRNAs. Total RNA from Ac₄ManNAz-labeled or label-free cells was extracted and purified by TRIzol as described above. For the Ac₄ManNAz-labeled cells, RNA was conjugated to DBCO-PEG4-biotin and precipitated as described above. The purification of biotin-labeled glycoRNAs was achieved by streptavidin beads with the following steps: 20 μL of MyOne C1 Streptavidin beads (Thermo Fisher Scientific) per reaction were blocked with 50 ng/ μL glycogen (Thermo Fisher Scientific) and 1 U/ μL RNase Inhibitor (NEB) in Biotin Wash Buffer (10 mM Tris HCl pH 7.4, 1 mM EDTA, 100 mM NaCl, 0.05% Tween-20) for 1 hour at 25°C. Next, 150 μg of the biotinylated total RNAs were diluted in 1 mL Biotin Wash Buffer and incubated with the blocked MyOne C1 beads for 4 hours at 4°C. Beads were washed to remove un-bound RNAs for three times with 1 mL of Biotin Wash Buffer each, followed by three washes with 1 mL of high salt Wash Buffer (10 mM Tris HCl pH 7.4, 1 mM EDTA, 500 mM NaCl, 0.05% Tween-20) each, then followed by three washes with 1 mL NaPO₄ Buffer (100 mM NaPO₄ pH 7.4) each, then followed by three washes with 1 mL of ChIRP Wash Buffer (2 \times SSC, 0.5% SDS) each, and finally by three washes with 1 mL NT2 Buffer (50 mM Tris HCl, pH 7.5, 150 mM NaCl, 1 mM MgCl₂, 0.005% NP-40). All washes were performed at 4°C for 10 minutes each. The streptavidin beads were then eluted by incubation in 1 mL TRIzol at 25°C for 10 minutes and the glycoRNA was extracted and purified as described above. The label-free glycoRNA enrichment was achieved by wheat germ agglutinin (WGA) agarose beads (Vector Laboratories), with the same blocking, incubation, washing, elution and purification steps as described above.

RNA and glycan fraction preparation from glycoRNAs

To release the glycan and RNA fractions from glycoRNAs, glycoRNAs were first purified on WGA beads as described above. GlycoRNAs on the WGA beads were digested with 7.5 μL PNGase F with GlycoBuffer 2 and 1 U/ μL RNase Inhibitor in a 100 μL volume at 37°C for 60 minutes. The RNA fraction was released and collected, followed by ethanol precipitation. The beads were washed with 200 μL Biotin Wash Buffer and high salt Wash Buffer. The glycan fraction on the WGA beads was then eluted by incubation with the Elution Buffer (Pierce, #1859690) for 10 minutes at room temperature on a tube rotator.

Flow cytometry

To test the binding of glycoRNAs to ECs and the effects of blocking P-/E-selectin, ECs were cultured and activated by TNF- α as described above. ECs were dissociated by enzyme-free cell dissociation buffer (Gibco), washed twice by HBSS with Ca²⁺ and Mg²⁺ and blocked with anti-P-selectin (Biolegend) or anti-E-selectin (eBioscience) antibodies at a dilution of 1:100 in HBSS with Ca²⁺ and Mg²⁺ at 37°C, 5% CO₂ for 10 minutes. Cells were washed by HBSS with Ca²⁺ and Mg²⁺. GlycoRNAs purified from Ac₄ManNAz-treated BM neutrophils were labeled with DBCO-PEG₄-biotin as described above. Biotin-labeled glycoRNAs were then reacted with Streptavidin-FITC. FITC-stained glycoRNAs or mock were incubated with ECs or with pre-blocked ECs at 37°C, 5% CO₂ for 10 minutes in HBSS with Ca²⁺ and Mg²⁺. Cells were washed twice by FACS buffer (PBS with 2% FBS), and analyzed on a BD LSR II flow cytometer. To test the interaction between glycoRNAs and selectins, recombinant P-selectin-Fc or E-selectin-Fc (Biolegend) were used to bind to live neutrophils. Neutrophil from BM underwent exRNaseA or mock treatment as described above. Neutrophils were incubated with P-selectin-Fc or E-selectin-Fc at a dilution of 1:100 in FACS buffer at 37°C, 5% CO₂ for 10 minutes. Neutrophils were washed twice by FACS buffer and incubated with a FITC-anti-Fc antibody (Sigma). The

levels of P-selectin and E-selectin binding signals were quantified using flow cytometry. To detect the Ac₄ManNAz labeling signal on the cell surface, Ac₄ManNAz treated WT or KD HOXB8 cells were labeled by DBCO-PEG4-biotin as described above. Cells underwent exRNaseA or mock treatment and were then incubated with Streptavidin-FITC. The biotin signals were quantified using flow cytometry.

Testing whether glycoRNAs were produced in a cell-intrinsic manner

Ac₄ManNAz-treated and mocked-treated BM neutrophils were stained by 1 μM CFSE and 1 μM Far-Red DDAO SE, respectively. The stained cells were then mixed at a 1:1 ratio, and co-cultured for 24, 48 and 72 hours in RPMI medium with 10% FBS, 1% penicillin-streptomycin and glutamine and 25 ng/mL GM-CSF. Of note, we did notice substantial cell death after 72 hours due to the life span of BM neutrophils in culture. Live neutrophils were then sorted, separated by the corresponding color using FACS. RNAs were extracted, biotin-labeled and blotted as described above.

Western blot analysis

For accessing KD or KO effects, western blot was performed using anti-Sid1 antibody (Thermo Fisher), anti-Sid2 antibody (Thermo Fisher), or anti-P-selectin antibody (Biolegend).

RT-qPCR

To confirm the enrichment of sequenced glycoRNAs, we performed RT-qPCR analyses. The poly adenylation of small RNAs and subsequent reverse transcription was performed using miRScript II RT KIT (QIAGEN). Quantitative PCR was performed using SYBR green PCR mix and with primers in [Table S3](#).

RNAseq analysis

Primary neutrophils were treated with exRNaseA or with mock treatment. Cells were washed by PBS for three times. Total RNAs from cells were extracted by TRIzol as described above. RNAseq library preparation via polyA selection and sequencing were performed by Yale Center for Genomic Analysis using standard Illumina kits, with the libraries sequenced on an Illumina NovaSeq sequencer.

GlycoRNA sequencing

Purified glycoRNAs were either used directly in small RNA library preparation, or first digested with PNGase F, repurified using TRIzol, and then subjected to small RNA library preparation. Of note, we did not notice substantial differences comparing sequencing results from PNGase F digested vs non-digested libraries. Library preparation follows our previously published procedure^{39,40} that follows identical steps as Illumina's TruSeq Small RNA Library Prep kit. The resultant libraries were sequenced by Yale Center for Genomic Analysis using an Illumina NovaSeq sequencer.

QUANTIFICATION AND STATISTICAL ANALYSIS

Sequencing data analysis

RNAseq reads were mapped to mouse genome assembly GRCm39 and normalized by DESeq2.

For glycoRNA sequencing analyses, data were obtained from our own sequencing experiment (for neutrophil and HOXB8 samples), or downloaded from GEO (GEO: GSE136967, for HeLa and H9 samples). Small RNA reads were analyzed using an in-house pipeline that we previously published,^{40,41} with a single step modification. Specifically, we updated our reference database for non-coding RNAs during the mapping process, now using Release 20 from the RNACentral database. We downloaded the genome coordinate files from the RNACentral database for both human (*homo_sapiens.GRCh38.gff3*) and mouse (*mus_musculus.GRCm39.gff3*). Reference noncoding RNA sequences were then extracted from the corresponding genome assemblies. We removed RNAs belonging to the categories of long noncoding RNAs, piRNAs, and misc sequences from the reference database, due to their frequent overlaps with other noncoding RNA species. We also added the 45S rRNA sequences from GenBank (NR_046233 for mouse, and NR_145819 for human) to the reference database due to their absence. This reference database was then used for mapping any sequence read equal or longer than 16 nt using Bowtie2. Unmapped reads were then mapped to the genome (mm10 for mouse and hg19 for human). Mapped reads in each sample were then normalized to reflect RPM (Reads per Million mapped reads). Significance of enrichment was assessed using Fisher's exact tests, comparing a purified sample vs the input control. Raw read counts for a given sequence in the two samples under comparison, as well as total mapped reads in the two samples minus the read count for the sequence under examination, were used in the test to derive p values. False discovery rate was then calculated based on the Benjamini and Hochberg method. For analysis of enriched glycoRNAs, such RNA sequences were defined as having FDR<0.05 and having at least 4-fold higher abundance in the glycoRNA samples than the control input sample.

Statistics

Student's t-test (unpaired, unequal variance) was used to assess experimental significance, unless specified otherwise.

Supplemental figures

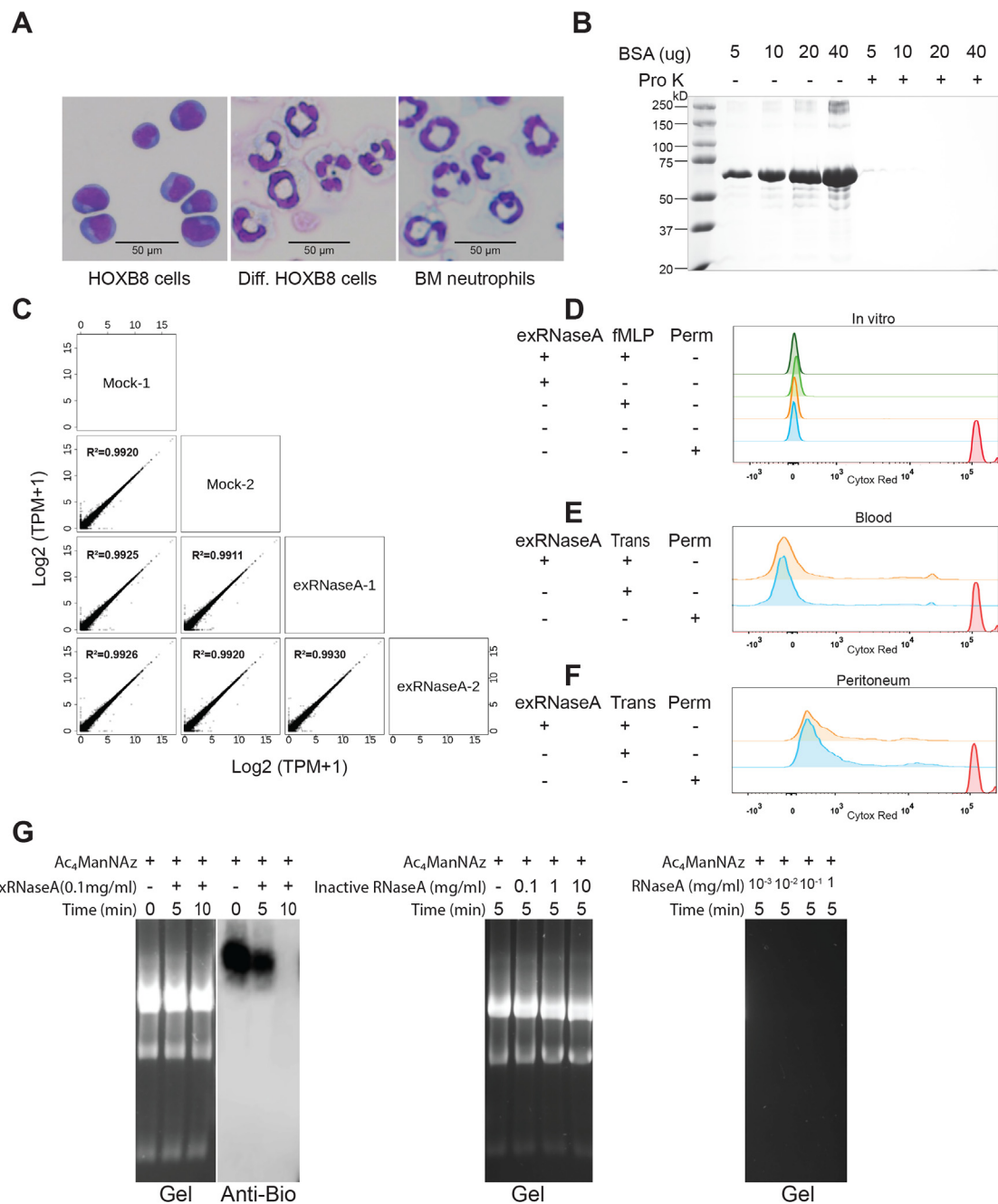


Figure S1. Enzymatic treatments of neutrophils and neutrophil RNAs, related to Figure 1

(A) HOXB8 cells, HOXB8-differentiated (Diff) neutrophils, and primary bone marrow neutrophils were cytospun onto slides and stained by the May Grunwald-Giemsa dyes. Representative microscopic images under bright field are shown.

(B) To test the activity of Pro K, BSA of the indicated quantities was used as a substrate and reacted with 2 mg/mL Pro K for 30 min at 37°C. Reactions were analyzed on an acrylamide gel, which was stained by Coomassie blue.

(C) Bone marrow neutrophils were treated with exRNaseA or with mock treatment, with two replicates each. RNAs were extracted and subjected to RNA-seq analysis. Each dot represents a gene. Data of transcripts per million (TPMs) are shown in log scale. R^2 values from Pearson correlation analyses are indicated.

(legend continued on next page)

(D) Primary bone marrow neutrophils were treated with mock or exRNaseA. Cells were then treated with vehicle control or fMLP *in vitro* and then incubated with Cytox Red (which stains cellular DNA when cell membrane integrity is impaired). As a positive control for Cytox Red staining, neutrophils were permeabilized (perm) before Cytox Red staining. Representative flow cytometry plots are shown.

(E and F) Primary bone marrow neutrophils were dye-labeled and treated with mock or exRNaseA. Recipient mice were conditioned by intraperitoneal injection (i.p.) of thioglycolate (TG) 1.5 h prior to transferring (Trans) neutrophils retro-orbitally (r.o.). Cells were harvested 2.5 h afterward from peripheral blood (E) and the peritoneum (F) and incubated with Cytox Red. Representative flow cytometry plots are shown. The positive Cytox Red control is the same as in (D).

(G) Left: bone marrow neutrophils were treated with Ac₄ManNAz and then with or without RNase A extracellularly (exRNaseA) at 0.1 mg/ml for the indicated minutes at 37°C. RNAs were extracted, reacted with DBCO-PEG₄-biotin, and analyzed on a gel followed by blotting with an anti-biotin antibody. Middle and right: RNAs purified from bone marrow neutrophils were digested with RNase A, inactivated RNase A, or mock, at the indicated concentrations for 5 min at 37°C. Reactions were analyzed on a gel. Both panels were cut from the same gel with the same exposure.

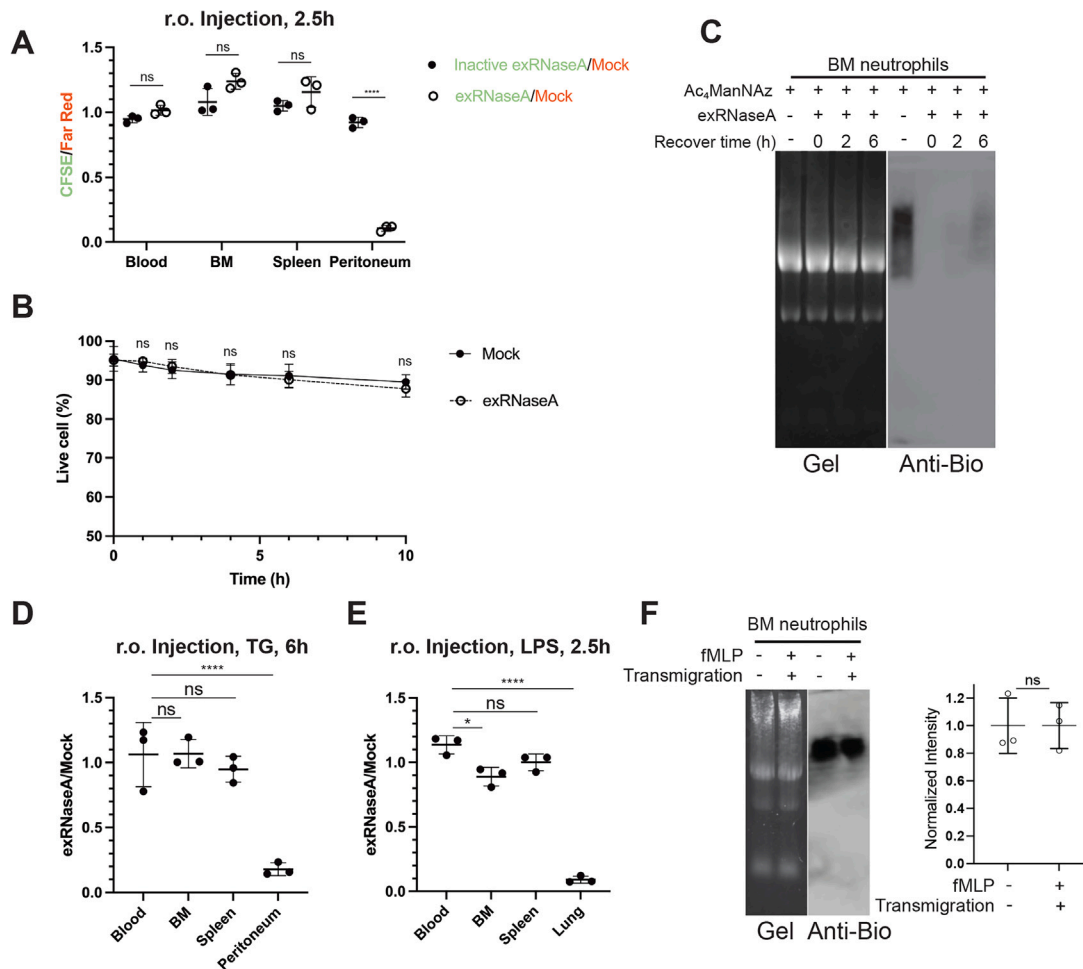


Figure S2. The effect of exRNaseA treatment on neutrophil recruitment *in vivo*, related to Figure 2

(A) Bone marrow neutrophils were labeled with a green (CFSE) or a far-red dye. Cells then underwent mock treatment or extracellular treatment by RNase A (exRNaseA) or inactivated RNase A (Inactive exRNaseA) before mixing test cells and control cells. Recipient mice were conditioned by intraperitoneal injection (i.p.) of thioglycolate (TG) 1.5 h prior to injecting the mixed neutrophils retro-orbitally (r.o.). Cells were harvested 2.5 h afterward from peripheral blood, bone marrow (BM), spleen, and peritoneum. Harvested cells were analyzed by flow cytometry, gating on Ly6G⁺ cells. The ratios between CFSE and far-red-labeled cells were plotted, with each dot representing a recipient mouse. *n* = 3. Data from a representative experiment are shown.

(B) Bone marrow neutrophils underwent mock treatment or extracellular treatment by RNase A (exRNaseA). Cells were cultured for the indicated amount of time. Cells were stained by trypan blue, and viable cells were counted and quantified.

(C) Bone marrow neutrophils were treated with Ac₄ManNAz and then with or without exRNaseA. Digested cells were then cultured in the presence of Ac₄ManNAz for the indicated amount of time before RNA harvest. RNAs were labeled with DBCO-PEG₄-biotin and analyzed on a gel followed by blotting with an anti-biotin antibody.

(D) A similar experiment as those in Figures 2A and 2B was performed, in which the mixture of mock and exRNaseA-treated bone marrow neutrophils was injected into mice preconditioned with the peritoneal TG treatment 1.5 h prior. Cells were harvested from the indicated tissues 6 h after injection. The ratio of exRNaseA-treated to mock-treated neutrophils was quantified and plotted. *n* = 3. Data from a representative experiment are shown.

(E) An acute lung inflammation model was used to test the effects of cell surface RNA removal. Recipient mice were preconditioned by intranasal LPS treatment for 16 h. Mock- and exRNaseA-treated bone marrow neutrophils were labeled with two different dyes and mixed before retroorbital (r.o.) injection into recipient mice. Cells from the indicated tissues were harvested 2.5 h afterward. The ratio of exRNaseA-treated to mock-treated neutrophils was quantified and plotted. *n* = 3. Data from a representative experiment are shown.

(F) Primary BM neutrophils were labeled with Ac₄ManNAz and then subjected to *in vitro* transwell migration, following the scheme in Figure 3A. Cells migrated to the bottom chamber were harvested after 2 h. These cells were compared with the same batch of Ac₄ManNAz-labeled neutrophils under control conditions without fMLP or migration. RNAs were harvested and analyzed for glycoRNA signals using the northern approach as in Figure 1A. Left: representative gel and blot. Right: quantification results. *n* = 3. For all panels, error bars represent standard deviations. **p* < 0.05; *****p* < 0.0001; ns: not significant.

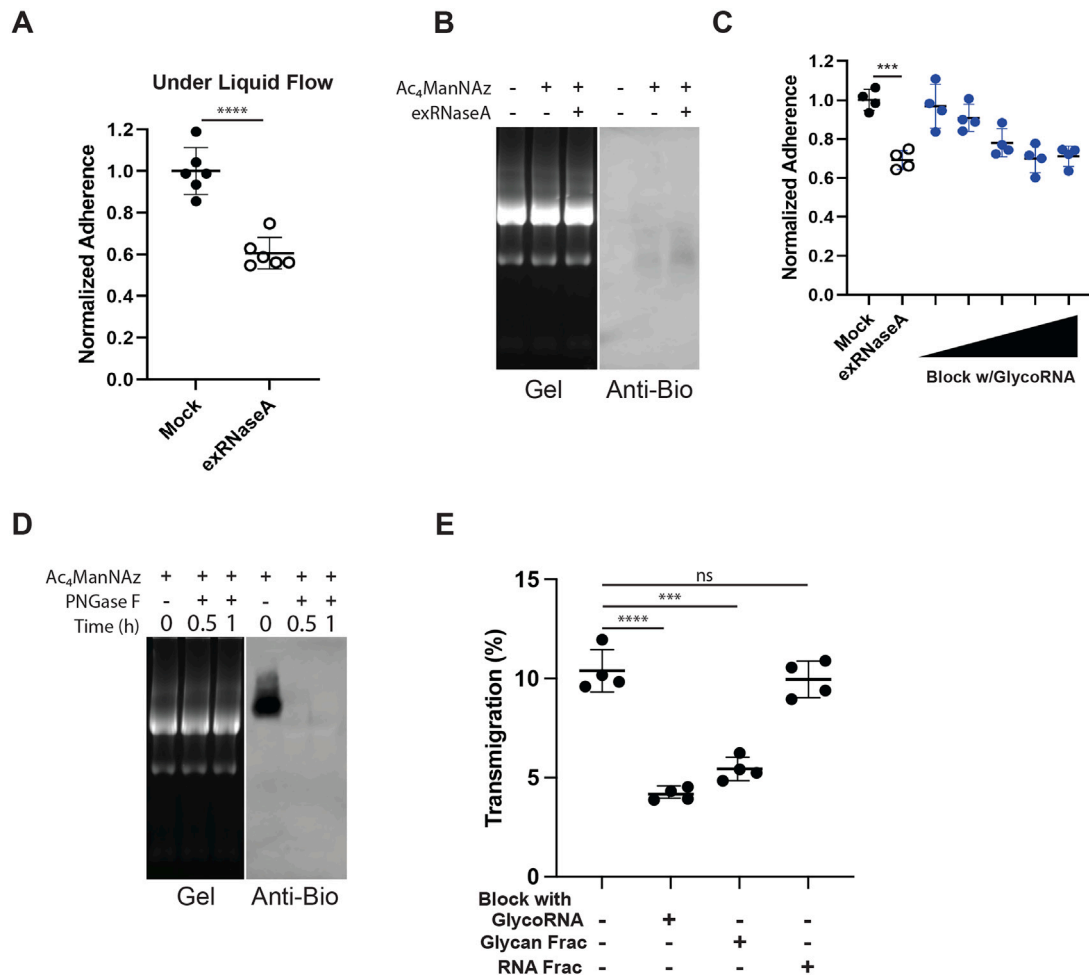


Figure S3. The effect of exRNaseA treatment on neutrophils' adhesion to and migration through endothelial cells, related to Figure 3

(A) Bone marrow neutrophils were treated with mock or exRNaseA, and neutrophils were analyzed for adherence to plated endothelial cells using a flow chamber with 2 dynes/cm² shear force. The adherence level was quantified as the number of neutrophils averaged across at least 12 random imaging fields along the flow path and normalized to the mock condition. n = 6 biological replicates.

(B) Endothelial cells were treated with or without Ac₄ManNAz and then treated with or without exRNaseA. Purified RNAs were then analyzed on a gel followed by blotting with an anti-biotin antibody.

(C) The saturating amount of glycoRNAs to block neutrophil adherence to endothelial cells (ECs) was tested. To prepare glycoRNAs, RNAs were extracted from bone marrow neutrophils, followed by purification using WGA beads. Plated ECs were pre-treated with increasing amounts of glycoRNA, representing materials from 0.1, 0.2, 0.5, 1, and 2 million bone marrow neutrophils. Bone marrow neutrophils were then analyzed for adherence to ECs following Figure 3B. As controls, mock- or exRNaseA-treated bone marrow neutrophils were analyzed on untreated ECs. n = 4.

(D) Bone marrow neutrophils were treated with Ac₄ManNAz. RNAs were harvested and treated with or without PNGase F for the indicated hours (h). Reactions were then analyzed on a gel followed by blotting with an anti-biotin antibody.

(E) An experiment related to Figure 3C was performed, in which ECs were plated on the transwell insert, and purified neutrophil glycoRNAs, the glycan fraction, or the RNA fraction was used to block ECs prior to testing the transendothelial migration by primary bone marrow neutrophils. The percentage of neutrophils that transmigrated within 2 h was quantified. For all panels, error bars represent standard deviations. ***p < 0.001; ****p < 0.0001; ns: not significant.

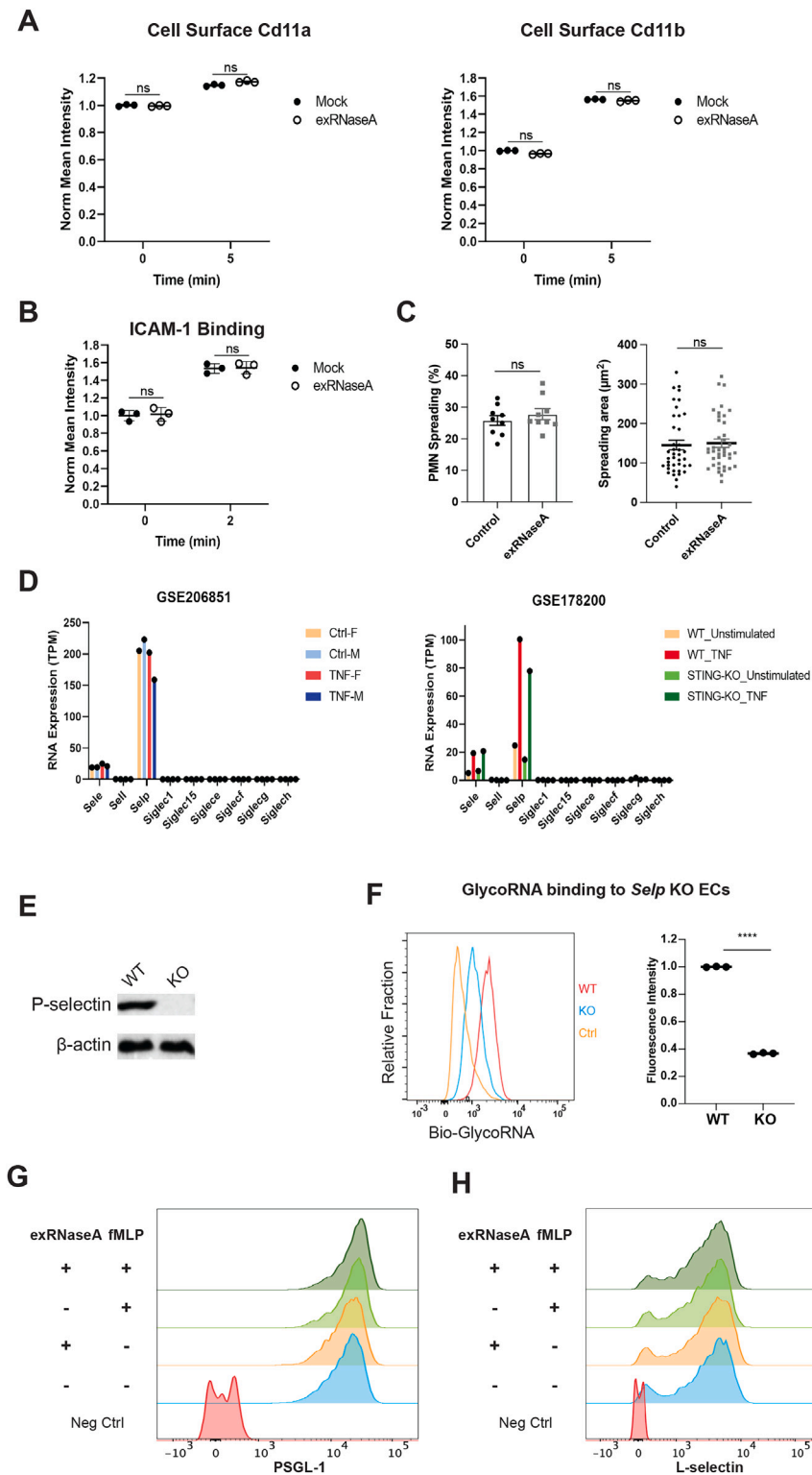


Figure S4. The identification of *Selp* as a receptor for neutrophil glycoRNAs, related to Figure 4

(A) Bone marrow neutrophils were treated with mock or exRNaseA, and then cells were treated with fMLP for the indicated amount of time. Cell surface Cd11a and Cd11b levels were determined by corresponding antibodies and analyzed by flow cytometry. Mean fluorescence intensities were normalized to those of the mock control. $n = 3$.

(B) Experiments were performed similar to (A), except that recombinant ICAM-1-Fc fusion protein was used to bind to cell surface. $n = 3$.

(legend continued on next page)

(C) Mock- (control) and exRNaseA-treated primary bone marrow neutrophils were assayed for their ability to spread on fibrinogen-coated surfaces. Left: the percentage of neutrophil displaying a spreading morphology was quantified, with nine dots representing data from three replicate wells and three random fields from each well. Right: the areas of spreading were quantified, with dots representing cells from the three replicates.

(D) Public RNA-seq data from the indicated GEO accession numbers were analyzed for the expression levels of the indicated lectin genes. In the left panel, male (M) and female (F) primary mouse aortic endothelial cells were treated with TNF- α or control (Ctrl). In the right panel, heart endothelial cells from wild-type or *Sting1* knockout (KO) with untreated or treated with TNF- α . Data were plotted in units of transcripts per million (TPMs).

(E) Endothelial cells (ECs) with *Selp* knockout (KO) were confirmed of the KO status using western blot.

(F) Biotin-labeled neutrophil glycoRNAs were purified and assayed for binding to WT and *Selp*-KO ECs. The levels of binding were quantified using flow cytometry after staining with fluorescently labeled streptavidin. Control cells were stained with fluorescently labeled streptavidin only. Left: representative flow cytometry plots are shown. Right: quantification results. $n = 3$.

(G and H) Primary bone marrow neutrophils were treated with mock or exRNaseA. Cells were then treated with vehicle control or fMLP. Levels of cell surface PSGL-1 and L-selectin levels were determined by corresponding antibodies. Representative flow cytometry plots are shown. For all panels except for (C), error bars represent standard deviation. For (C), error bars represent SEM. **** $p < 0.0001$; ns: not significant.

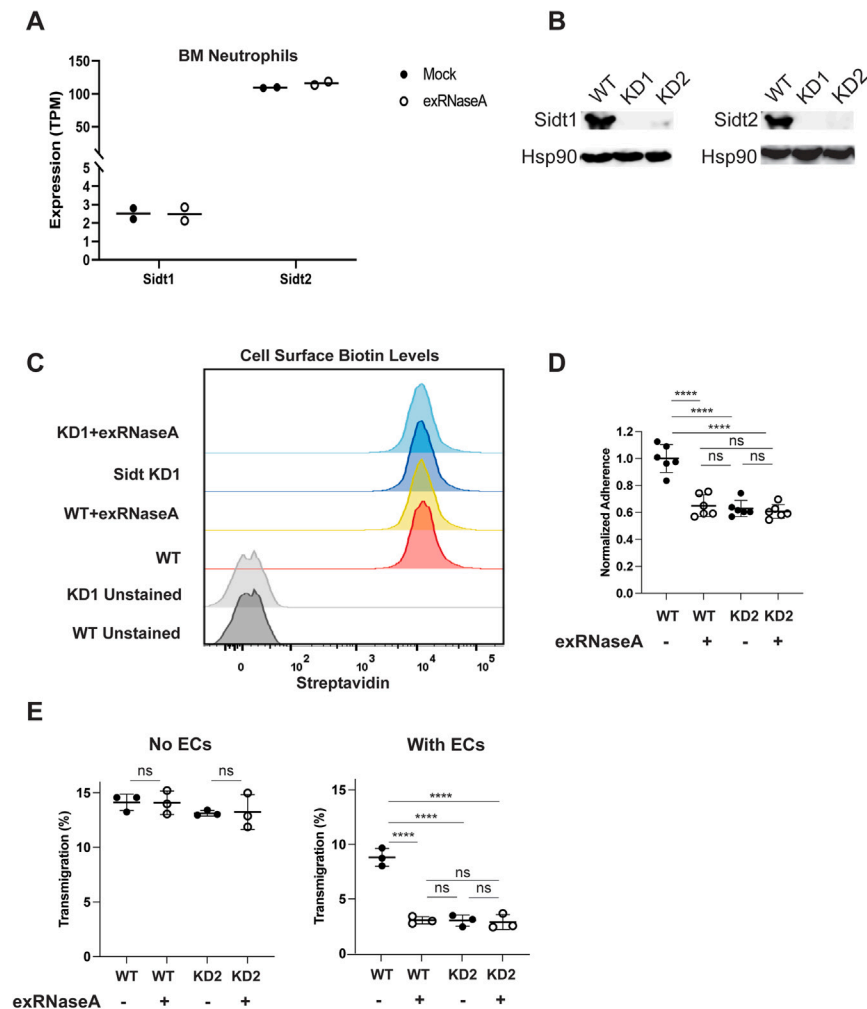


Figure S5. The effects of *Sidt* knockdown in HOXB8 cells, related to Figure 5

(A) The RNA expression levels of *Sidt1* and *Sidt2* were plotted from the RNA-seq data in Figure S1C, in units of transcripts per million (TPMs).

(B) HOXB8 cells immortalized from a Cas9 mouse were transduced with two independent sets of sgRNAs to knockdown (KD) the expression of both *Sidt1* and *Sidt2*. Western blot analyses were performed to evaluate the KD efficiency.

(C) Control Cas9-expressing HOXB8 cells (Ctrl) or *Sidt* KD HOXB8 cells were treated with Ac₄ManNAz, followed by direct click-chemistry reaction with DBCO-PEG₄-biotin to label cell surface glycans incorporated with Ac₄ManNAz. Cells then underwent mock or exRNaseA treatment. Biotin levels on cell surface were then analyzed by streptavidin binding and flow cytometry. Representative flow cytometry plots are shown.

(D) Neutrophils differentiated from wild-type (WT) and KD HOXB8 cells with sgRNA vector 2 (KD2) were subjected to exRNaseA or mock treatment. Cells were analyzed for adherence to endothelial cells (ECs) similar to Figure 3B. Each dot represents a biological replicate. n = 6. Data from a representative experiment are shown.

(E) Cells in (D) were analyzed for transmigration with or without ECs, similar to experiments in Figure 3A. Each dot represents a biological replicate. n = 3. Data from a representative experiment are shown. For all panels, error bars represent standard deviation. ***p < 0.001; ****p < 0.0001; ns: not significant.

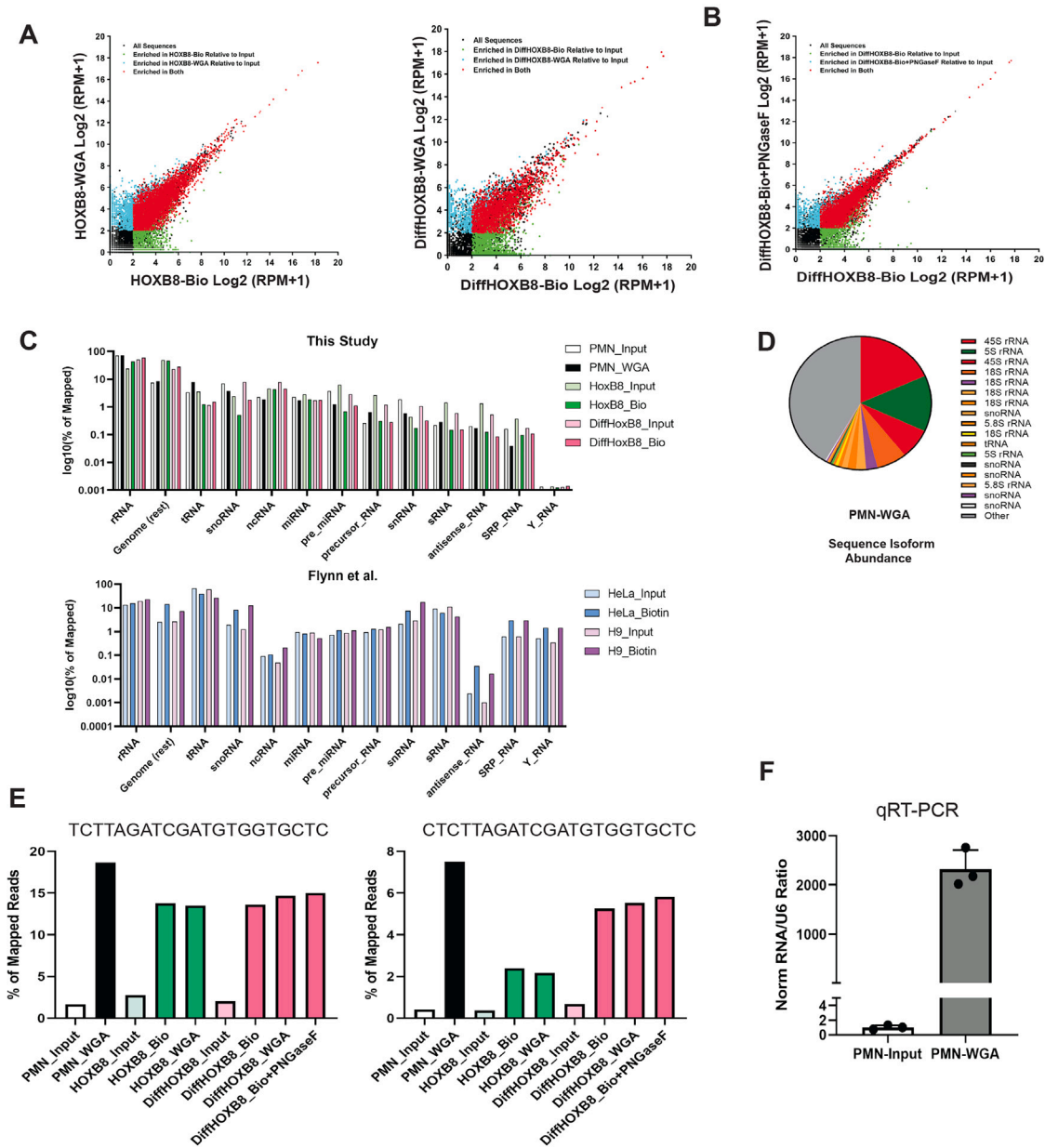


Figure S6. Analyses of neutrophil glycoRNA sequences, related to Figure 6

(A and B) Small RNA sequencing reads from the purified glycoRNA fractions or the control input samples were mapped to the RNA Central database and the genome. Data were normalized to reflect reads per million mapped reads (RPM). Significance of enrichment for each sequence was calculated in comparison to the same read in the corresponding input small RNA library. Scatter plots are shown for comparison between the indicated samples. Each dot represents one sequence. Sequence isoforms were plotted as separate dots. Significantly enriched sequences (false discovery rate [FDR] < 0.05, fold change compared with input ≥ 4) were colored according to the legends.

(C) The percentage of reads mappable to the indicated RNA categories was shown for murine samples in this study as well as for the published data of human H9 and HeLa cell lines (from Flynn et al.).

(D) The fractions of the top enriched sequence isoforms among all mapped reads were plotted for the PMN-WGA sample. Each pie represents one sequence, with the exception that the last “other” pie represents all remaining sequences. Sequence isoforms were plotted as separate pies. The annotation on the right indicates the RNA species that the sequence read was best mapped to.

(E) The top and third most abundant sequence isoforms belong to the same small RNA mappable to the 5' end of 45S rRNA. The sequences are indicated on top of the graph. The abundance of the reads across the indicated libraries was plotted as the percent of all mapped reads.

(F) RT-qPCR was performed to validate the enrichment of the small RNA in (D). The levels of both the 45S-rRNA-derived glycoRNA and U6 small RNA (depleted during purification) were measured in input total RNA and in WGA-purified RNA from primary neutrophils (PMNs). Data represent the ratios between the two and were normalized (norm) by the input levels. n = 3. Error bars represent standard deviation.